

# NASA-DOD LEAD-FREE ELECTRONICS PROJECT: VIBRATION TEST

Thomas A. Woodrow, Ph.D.  
Boeing Research and Technology  
Seattle, WA  
thomas.a.woodrow@boeing.com

## ABSTRACT

Vibration testing was conducted by Boeing Research and Technology (Seattle) for the NASA-DoD Lead-Free Electronics Solder Project. This project is a follow-on to the Joint Council on Aging Aircraft/Joint Group on Pollution Prevention (JCAA/JG-PP) Lead-Free Solder Project which was the first group to test the reliability of lead-free solder joints against the requirements of the aerospace/military community.

Twenty seven test vehicles were subjected to the vibration test conditions (in two batches). The random vibration Power Spectral Density (PSD) input was increased during the test every 60 minutes in an effort to fail as many components as possible within the time allotted for the test.

The solder joints on the components were electrically monitored using event detectors and any solder joint failures were recorded on a Labview-based data collection system. The number of test minutes required to fail a given component attached with SnPb solder was then compared to the number of test minutes required to fail the same component attached with lead-free solder.

A complete modal analysis was conducted on one test vehicle using a laser vibrometer system which measured velocities, accelerations, and displacements at one hundred points. The laser vibrometer data was used to determine the frequencies of the major modes of the test vehicle and the shapes of the modes. In addition, laser vibrometer data collected during the vibration test was used to calculate the strains generated by the first mode (using custom software).

After completion of the testing, all of the test vehicles were visually inspected and cross sections were made. Broken component leads and other unwanted failure modes were documented.

Key Words: vibration, lead-free solder, NASA, reliability

## INTRODUCTION

The NASA-DoD Lead-Free Electronics Project was started in 2006 to determine whether lead-free solders and finishes (before and after rework) are suitable for use in high reliability electronics. The Project is managed by NASA. The NASA-DoD Lead-Free Electronics Project includes members from the U.S. Air Force, BAE Systems,

Boeing, Celestica, Harris, Lockheed Martin, NASA, NAVSEA Warfare Centers (Crane), Raytheon, Rockwell-Collins, ACI, Lockheed Martin, and Texas Instruments, among others. This project is a follow-on to the 2001 Joint Council on Aging Aircraft/Joint Group on Pollution Prevention (JCAA/JG-PP) Lead-Free Solder Project which was the first group to test the reliability of lead-free solder joints against the requirements of the aerospace/military community.

The Project members wrote a Project Plan [1] which describes the assembly of the test vehicles and the testing to be done. The testing includes thermal cycling, vibration, mechanical shock, combined vibration/thermal cycling, and copper dissolution testing.

The objective of this study was to determine the effects of random vibration on the relative reliability of as-assembled and reworked lead-free and tin/lead solder joints (i.e., which solder survived the longest). Modal data and strain data were also collected during this study in an effort to provide data that would be useful to those that may want to try to model the behavior of the NASA-DoD test vehicle.

## APPROACH

The test vehicle designed for this project was a six-layer circuit board 12.75 inches wide by 9 inches high by 0.090 inches thick (32.39 cm by 22.86 cm by 0.23 cm) (Figure 1). The design used 0.5 ounce copper and a laminate with a high glass transition temperature ( $T_g$  of 170 degrees C, Isola 370HR). The test vehicle was populated with 63 components consisting of ceramic leadless chip carriers (CLCC's), QFN's, Alloy 42 TSOP's, TQFP's, BGA's, CSP's, and PDIP's. The components contained internal wire bonds so that once mounted on the test vehicle, each component would complete an electrical circuit that could be monitored during testing. Failure of a solder joint would cause a break in the electrical circuit that could be detected by an event detector. Each test vehicle also had a daisy-chain of twelve 0.016 inch (0.041 cm) diameter plated through holes so that the reliability of the holes could be determined. The plated through holes were filled with solder during the wave solder operation. Each component location on the test vehicles was given a unique reference designator number.

The solder alloys selected for test were:

**Sn3.0Ag0.5Cu** paste for reflow soldering (abbreviated as SAC305)

**Sn0.7Cu0.05Ni** for wave soldering and as a paste for reflow soldering (abbreviated as SN100C)

**Sn37Pb** for reflow and wave soldering (abbreviated as SnPb)

**Sn4.0Ag0.5Cu** for BGA balls (abbreviated as SAC405)

**Sn1.0Ag0.5Cu** for CSP balls (abbreviated as SAC105)

The SAC305 alloy was chosen because it is currently the preferred alloy for use in lead-free commercial electronics. The SN100C alloy was chosen because it has been widely used around the world with good results. SAC405 and SAC105 are alloys commonly used in the balls on area array devices. Finally, eutectic SnPb was included to act as the control alloy.

The test vehicles were divided into two types, i.e., “Manufactured” test vehicles and “Rework” test vehicles. Both types were made using an immersion silver board finish (although an ENIG PWB finish was used on a few of the test vehicles). The lead-free “Manufactured” and “Rework” test vehicles were assembled using lead-free solders and lead-free reflow and wave soldering profiles. The SnPb “Manufactured” and “Rework” test vehicles were assembled using eutectic SnPb solder and SnPb reflow and wave soldering profiles and were used as the controls. A 5-mil laser cut stencil was used during paste application.

As the name suggests, selected components on the “Rework” test vehicles were reworked. The components were removed; residual solder was cleaned from the pads using solder wick; and new components were attached using either SnPb or lead-free solder.

The “Rework” test vehicles were also populated with a number of mixed technology components (i.e., SnPb paste combined with a lead-free component finish or lead-free paste combined with a SnPb component finish).

The CLCC’s with a lead-free pad finish were produced by dipping of gold-plated CLCC’s into the respective molten solders. In addition, some tin-plated TQFP’s were dipped into either molten SnPb or molten SAC305 to simulate a tin whisker mitigation process.

The component finishes used included SnPb, matte Sn, SnBi, SAC305, SAC405, and SAC105.

Table 1 lists the components used on the SnPb and lead-free “Manufactured” test vehicles; the finish on each component; and the solders used.

Table 2 lists the components used on the SnPb and lead-free “Rework” test vehicles; the finish on each component; the solders used; and which components were actually reworked.

One hundred and ninety three test vehicles were assembled at BAE Systems in Irving, TX. One hundred

and twenty of these test vehicles were “Manufactured” PWA’s and seventy three were “Rework” PWA’s. Eighteen components were reworked on each of the “Rework” test vehicles (six BGA’s; six CSP’s; two PDIP’s; and four TSOP’s). In general, solder wire was used for reworking the components. The BGA’s and CSP’s, however, were replaced using flux only or by applying paste to the balls and then using a hot air rework station to form the solder joints (see Table 2). During rework of the BGA’s and CSP’s, a SnPb thermal profile was used for the SnPb “Rework” test vehicles and a Pb-free thermal profile was used on the Pb-free “Rework” test vehicles. The reflow profiles for initial assembly using either SnPb or the lead-free solder pastes are shown in Figures 2 and 3. The wave soldering profiles used for tin/lead and lead-free wave soldering can be found in [2]. Wave soldering with SnPb was done at BAE Systems and the lead-free wave soldering was done at Scorpio Solutions in Garfield Heights, Ohio. The rework profiles for removing and replacing the BGA’s and the CSP’s using a hot air rework station can also be found in [2]. All rework was done at BAE Systems, Lockheed Martin, and Rockwell-Collins. Each rework site focused on the test vehicles for a specific test to eliminate effects due to site-to-site variations in rework procedures.

After assembly and rework, all test vehicles were thermally aged at 100°C for 24 hours. Twenty seven test vehicles were then delivered to Boeing for mechanical shock testing. These consisted of 5 SnPb “Manufactured” test vehicles; 6 Pb-free “Manufactured” test vehicles assembled with SAC305 paste; 5 Pb-free “Manufactured” test vehicles assembled with SN100C paste; 6 SnPb “Rework” test vehicles; and 5 Pb-free “Rework” test vehicles. All of the test vehicles had an immersion silver PWB finish except for one SAC305 “Manufactured” test vehicle (Test Vehicle 96) and one SnPb “Rework” test vehicle (Test Vehicle 157) which had an ENIG PWB finish.

On the SnPb “Rework” test vehicles, all of the CLCC’s were finished with SAC305 (on the pads and in the castellations) and assembled with SnPb paste which resulted in lead-free solder joints contaminated with Pb after assembly (see Table 2). In addition, some of the BGA’s combined SAC405 balls with SnPb solder paste which resulted in lead-free solder joints contaminated with Pb (on reworked and unreworked BGA’s). Also, some of the CSP’s combined SAC105 balls with SnPb solder paste (reworked and unreworked). This mixing was done intentionally in order to determine the effects of lead-contamination upon lead-free solder reliability. Inductively coupled plasma (ICP) spectroscopy was used by Boeing to quantify the amount of Pb in these solder joints on one of the SnPb “Rework” test vehicles (see Table 3; Test Vehicle ID # 149). The solder joints were removed with a scalpel, dissolved in mixed nitric/hydrochloric acid, and the solution was analyzed by ICP spectroscopy.

On the Pb-free “Rework” test vehicles, all of the CLCC’s and QFN’s were finished with SnPb and assembled with SAC305 paste which resulted in lead-free solder joints contaminated with Pb after assembly (see Table 2). In addition, some of the BGA’s combined SnPb balls with SAC305 solder paste which

resulted in lead-free solder joints contaminated with Pb (on unreworke BGA's). Also, some of the CSP's combined SAC105 balls with SnPb solder paste (after rework). This mixing was done intentionally in order to determine the effects of lead-contamination upon lead-free solder reliability. Again, inductively coupled plasma (ICP) spectroscopy was used by Boeing to quantify the amount of Pb in these solder joints on one of the Pb-Free "Rework" test vehicles (see Table 3; Test Vehicle ID # 193).

All of the ICP analyses appeared reasonable with the possible exception of the two TSOP's and the BGA U43 analyses. The copper content for these components were higher than expected. It is probable that copper was removed from the test vehicle pads along with the solder when the solder joints were cut from the test vehicle using a scapel.

An aluminum fixture was built that could hold up to fifteen test vehicles at one time. Slots were cut into the fixture to accept wedgelocks (Calmark A260-8.80T2L) that were mounted on both ends of the test vehicles with screws. The wedgelocks were designed with a special locking feature to prevent loosening from vibration and were torqued to 8.5 in-lbs. Figures 4 and 5 show the NASA-DoD test vehicles mounted in the test fixture.

The electrodynamic shaker used for the test was an Unholtz-Dickie T1000W with a 360 KW amplifier controlled by a Spectral Dynamics 2550B Vibration Controller. The shaker input was controlled by three accelerometers mounted on the fixture.

An understanding of the bending modes of the NASA-DoD test vehicle is important since the vibration input should excite these bending modes which in turn will cause solder joint damage.

A modal analysis was conducted on the test vehicle located in the end slot of the test fixture using a laser vibrometer system (Polytec Scanning Vibrometer, Waldbronn, Germany). The end of the fixture was removed during the modal analysis so the vibrometer could scan the test vehicle. The laser vibrometer was used to measure velocities, accelerations, and displacements at 100 points on the bottom surface of Test Vehicle 74 during low level random vibration in the z-axis (the axis perpendicular to the plane of the test vehicle). The laser vibrometer measurements identified 3 major resonance frequencies for the NASA-DoD test vehicle at 65, 390, and 980 Hz. The laser vibrometer data was also used to calculate a bending mode shape for each of the resonances (see examples in Figures 6 and 7).

Most of the "Manufactured" and "Rework" test vehicles were instrumented with two calibrated accelerometers as shown in Figure 1 for collecting acceleration data during the vibration test. Accelerometer 1 was located at the

point of maximum deflection for the first and second modes (65 and 91 Hz) and Accelerometer 2 was located at the point of maximum deflection for the seventh mode (390 Hz). The transmissibilities (Q's) for the major modes as measured by each of the accelerometers at each test level were recorded.

Four three-element stacked rosette strain gages were mounted on one test vehicle as shown in Figure 8 to collect strain data in the x and y directions at each test level (directions are defined in Figure 1).

Figures 9 through 10 show the transmissibilities and the displacements of a test vehicle vs. frequency (from accelerometer data collected during a 1 G sine sweep of a "Manufactured" test vehicle in the z-axis). Figure 10 illustrates that the most displacement (and therefore the most solder joint damage) is caused by the first resonance. The resonance near 390 Hz caused approximately 69 times less displacement than the first resonance at the location of Accelerometer 1.

Figure 11 shows rms strain vs. frequency as measured by two of the strain gages mounted on Test Vehicle 74 (in the x-direction during the 8.0 Grms test). This data demonstrates that the magnitude of the strain is location dependent. Also note that down the centerline of the test vehicle (Strain Gage 4), the strains are produced predominately by the first mode while at the location of Strain Gage 3, the strains produced by the first and seventh modes are nearly equivalent.

The data in Figure 11 clearly demonstrates that the strain environment at a given location on a test vehicle can be very different from the strain environment at a different location on the same vehicle during the same test. This implies that the best practice is to directly compare identical components in identical locations on identical test vehicles. It also implies that the test solder must be used on one set of test vehicles and the control solder on a second set of test vehicles.

Laser vibrometer velocity data was also collected at 100 points on the surface of Test Vehicle 74 during a one G sine dwell at the first mode frequency. This data was used to calculate full field peak strains in the vehicle x direction for the first mode (see Figure 12). The calculations were performed using Boeing proprietary software. The regions of calculated maximum strain were down the centerline of the vehicle and along the edges of the vehicle (near the wedgelocks). Note that the strains shown in Figure 12 are compressive down the centerline of the test vehicle and tensile along the edges of the vehicle. When the board bends in the opposite direction the compressive strains will become tensile and the tensile strains will become compressive.

After collection of the modal and strain data, the test vehicles were subjected to a random vibration step stress test in the z-axis only (see Figure 13 and Table 4). The 27 test vehicles were divided into two groups for testing. The first group contained most of the "Manufactured" test vehicles. The

second group contained all of the “Rework” test vehicles and the balance of the “Manufactured” test vehicles.

The test started with one hour of vibration at 8.0 Grms in the z-axis (the axis perpendicular to the plane of the PWA). This was followed by one hour of vibration at 9.9 Grms and then one hour of vibration at 12.0 Grms. The vibration levels were then increased in 2.0 Grms increments, shaking at each level in the z-axis for one hour until completion of the 20.0 Grms run (i.e., a step stress test). The test was completed with one hour of vibration at 28.0 Grms in the z-axis.

Figure 14 shows the shaker input into the test vehicle fixture and Figure 15 shows the typical response of a test vehicle (both during an 8.0 Grms run). Note that the response of the test vehicle differs greatly from the input PSD spectrum with the major test vehicle resonances occurring at 67.5 Hz and 395 Hz.

The 63 components and the PTH net on each test vehicle were individually monitored using Analysis Tech 256STD Event Detectors (set to a 300 ohm threshold) combined with Labview-based data collection software. The wires connecting the test vehicle to the event detector had to be glued to the surface of the test vehicle (Figure 1) to prevent them from flexing and breaking during the vibration test. In addition, the wire bundles from the test vehicle were firmly clamped to the fixture in order to prevent flexing and breaking of the wires. All wire bundles were covered with a grounded metallic shield to prevent electrical noise from the shaker from interfering with the event detectors.

## RESULTS AND DISCUSSION

Table 5 shows the percent of each component type that failed on both the “Manufactured” and the “Rework” test vehicles at the end of the test. Notice that the QFN-20’s were resistant to failure due to vibration.

Figure 16 shows when the components failed on Test Vehicle 74. The failures are colored coded according to which how many test minutes were required to cause the failure (red = 1 to 60 test minutes; orange = 61 to 120 minutes; yellow = 121 to 180 minutes; green = 181 to 240 minutes; blue = 241 to 300 minutes; purple = 301 to 360 minutes; pink = 361-420 minutes; and white = 421 to 480+ minutes). In general, the components tended to fail first down the centerline and along the edges of the test vehicle (near the wedgelocks). Therefore, the first component failures coincide with the regions of highest strain as shown in Figure 12.

After completion of all vibration testing, the “Manufactured” and “Rework” test vehicles were visually inspected using a HYROX Hi-Scope Compact Micro Vision System (Model KH-2200 MD2). The main goal of the inspection was to document any broken or missing leads on leaded components. This was necessary so that

failures due to solder joint cracking could be distinguished from failures due to lead breakage. The secondary goal of the inspection was to document any unusual failure modes. The complete visual inspection results for each test vehicle can be found in [2]. Some components (BGA’s and TSOP’s) tended to fall off of the test vehicles during testing. In addition, all wiring was visually inspected to verify that no signal wires had broken during the vibration test (a broken signal wire would look like a solder joint failure to the event detectors). No broken signal wires were found.

Microsections were also done to identify major failure modes. For the BGA’s and CSP’s, microsections were done on components that failed late in the test in the hope that it would be easier to determine the true failure mechanism since secondary failure mechanisms might not yet have had time to develop.

At the end of the test, numerous components had failed electrically which allowed the relative reliability of the SnPb control solder and the lead-free solders to be compared.

The percentage of each component population that failed was plotted against the accumulated vibration test minutes. Each of the plots groups data from components that were assembled using the same solder alloy/component finish combinations. For example, all of the BGA’s in positions U4, U5, and U55 (Figure 17) used SnPb solder/SnPb balls on the SnPb “Manufactured” test vehicles; SAC 305 solder/SAC405 balls and SN100C/SAC405 balls on the Pb-Free “Manufactured” test vehicles; SnPb solder/SAC405 balls on the SnPb “Rework” test vehicles; and SAC 305 solder/SnPb balls on the Pb-Free “Rework” test vehicles. The plots in Figure 17 allow a direct comparison between the combined failures of all of these BGA’s even though they were in different strain environments during the test.

The overall results of the vibration testing (from the data plots) are summarized in Table 6. If a solder alloy/component finish combination performed as well or better than the SnPb control, it was assigned the number “1” and the color “green”. Solders that performed worse than the SnPb control were assigned a “2” and the color “yellow”. Solders that performed much worse than the SnPb control were assigned a “3” and the color “red”.

The rankings in Table 6 are somewhat subjective due to the scatter in the data for some component types. The TSOP data was difficult to interpret since the orientation of the TSOP on the test vehicle appeared to influence how the solder/component finish combinations performed relative to the Sn37Pb/SnPb controls. Weibull plots were not used since the test conditions were changed during the test (i.e., the PSD was increased every 60 minutes) which renders the Weibull parameters meaningless.

In the following sections, the solder paste used is listed first followed by the component finish (for example,

SAC305/SAC405 on a BGA is equivalent to SAC305 solder/SAC405 balls).

#### **BGA-225's**

The combination of SAC305 solder/SAC405 balls and SN100C/SAC405 balls performed poorly when compared to the SnPb/SnPb controls in vibration (see Figures 17, 18, and 19). This is consistent with the results of the earlier JCAA/JG-PP study [3].

Microsections made at the end of the test showed that the corner solder joints failed first. The SnPb/SnPb sections showed solder joint cracking on both the component side and the PWB side of the joints (Figure 20). The SAC305/SAC405 sections showed a number of trace cracks on the component side, PWB trace cracking, and some voiding (see Figures 21 and 22).

The combination of SAC305 solder/SnPb balls and SnPb solder/SAC405 balls also performed poorly compared to the SnPb/SnPb controls (Figure 17) on either an immersion silver or ENIG board finish. The SnPb/SAC405 BGA's were reflowed using a SnPb reflow profile. The SnPb/SAC405 microsections showed solder joint cracking on the PWB side of the solder joints and trace cracking on the component side (see Figure 23).

SnPb/SnPb BGA's reworked with flux only/SnPb balls and SAC305/SAC405 BGA's reworked with flux only/SAC 405 balls were much less reliable than the SnPb/SnPb control BGA's (Figure 18).

SnPb/SnPb BGA's reworked with SnPb/SAC405 and SAC305/SAC405 BGA's reworked with SnPb/SAC405 also underperformed the SnPb/SnPb controls (Figure 19). The former were reworked with a SnPb thermal profile while the latter were reworked with a Pb-free thermal profile which should have facilitated mixing of the solders.

During rework of the BGA's, problems were encountered with electrical opens. This required that six BGA's be reworked several times instead of just once. See [2] to determine which BGA's were reworked multiple times. In general, the BGA's that were reworked multiple times performed approximately the same as those that were reworked just once.

A few SnPb/SnPb BGA's and SAC305/SnPb BGA's fell off of the test vehicles during the vibration test which allowed the failure mechanisms to be examined more closely. The missing BGA's were on test vehicles with an immersion silver board finish.

On the SnPb/SnPb BGA's that fell off, most of the failures occurred on the package side (Figure 24). Most of the balls were still present (80.9 to 84.0 percent of the total balls). About half of the missing balls were also missing the associated pads (44.2 to 52.6 percent).

On the SAC305/SnPb BGA's that fell off, most of the failures also occurred on the package side. Most of the balls were still present (94.7 to 96.9 percent of the total balls). Many of the missing balls were also missing the associated pads (33.3 to 100 percent). Voiding was also observed.

No missing BGA's were seen for the other solder/BGA ball combinations.

#### **CLCC-20's**

The SnPb/SnPb controls outperformed the combinations of SAC305/SAC305, SN100C/SAC305, SnPb/SAC305, and SAC305/SnPb (See Figure 25).

The amount of Pb detected in the SnPb/SAC305 and SAC305/SnPb solder joints was 24.7% and 16.5%, respectively (from ICP spectroscopy, see Table 3).

Figure 26 shows a crack typical of those found in the CLCC solder joints.

#### **CSP-100's**

The CSP daisy chain pattern on the test vehicles was incorrect with the result that only the outer perimeter balls of each CSP formed an electrically continuous path. In order for a CSP to be detected as failed, both legs of the outer perimeter needed to fail.

The combination of SAC305 solder/SAC105 balls and SN100C/SAC105 balls generally performed as well as the SnPb/SnPb controls in vibration (see Figures 27 through 29). Microsections made at the end of the test showed that the corner solder joints failed first. Both the SnPb/SnPb and the SAC305/SAC105 solder joints formed cracks on the component side of the CSP's (Figure 30).

The combination of SAC305 solder/SnPb balls slightly underperformed the SnPb/SnPb controls (Figure 27). In contrast, the combination of SnPb solder/SAC105 balls outperformed the SnPb/SnPb controls (Figure 27). These SnPb/SAC105 components were reflowed using a SnPb reflow profile.

The SnPb/SnPb CSP's reworked with flux only/SnPb balls were about as reliable as the SnPb/SnPb control CSP's while the SAC305/SAC105 CSP's reworked with flux only/SAC 105 balls underperformed the SnPb/SnPb control CSP's (Figure 28).

SnPb/SnPb CSP's reworked with SnPb/SAC105 performed about as well as the SnPb/SnPb controls but the SAC305/SAC105 CSP's reworked with SnPb/SAC105 greatly underperformed the SnPb/SnPb controls (Figure 29). The former were reworked with a SnPb thermal profile while the latter were reworked with a Pb-free thermal profile which should have allowed complete mixing of the solders.

### **PDIP-20's**

The combinations of SN100C solder/Sn component finish and SN100C solder/NiPdAu component finish underperformed the SnPb/SnPb and SnPb/NiPdAu controls in vibration (see Figure 31). These results are in sharp contrast to the results from the JCAA/JG-PP Lead-Free Solder Project [3] in which SN100C solder/Sn outperformed SnPb/Sn and SN100C solder/NiPdAu outperformed SnPb/NiPdAu.

The SnPb/SnPb PDIP's reworked with SnPb/Sn outperformed the SN100C/Sn PDIP's reworked with SN100C/Sn but both were much less reliable than the unreworked SnPb/SnPb control PDIP's (Figure 32). These results for the reworked PDIP's are more in line with the results from the JCAA/JG-PP study [3].

Microsections made at the end of the present study showed that the PDIP corner solder joints near the wedgelocks failed before the other PDIP solder joints. On both the SnPb and SN100C joints, the topside solder fillet would crack first followed by cracking of the lead where it necks down at the top of the PTH (see Figure 33).

The reasons for the very different PDIP test results from this study and the JCAA/JG-PP study are not clear. The test vehicles, test equipment, and test procedures for the two tests were almost identical. Microsections done for the current study revealed only the expected cracking of the solder joints/leads in the PDIP corner positions and no unusual failure mechanisms such as barrel cracking of the PTH's were observed. However, a visual inspection revealed that the PDIP's soldered with SN100C had many more trace cracks next to the PDIP corner solder filets near the wedgelocks than did the PDIP's soldered with SnPb (see Figure 34). Probing with an ohmmeter showed that 4 out of 25 SnPb PDIP's exhibited possible trace cracking at the end of the test compared to 42 out of 60 SN100C PDIP's which exhibited possible track cracking. One possible explanation is that the copper on the NASA-DoD test vehicles was not as ductile as that used on the JCAA/JG-PP test vehicles which resulted in a new failure mechanism. In areas of high board strain, the PDIP's soldered with SN100C might cause the traces to crack resulting in early failures while the PDIP's soldered with SnPb might not cause trace cracking due to the difference in the material properties (modulus, etc.) of the two solders. Interestingly, the data for PDIP U59 indicated that SnPb solder and SN100C solder were equivalent in performance except on Test Vehicles 112 and 115 which failed early and also exhibited cracked traces. This suggests that at least some of the early failures observed in this test were due to trace cracking. In addition, the two SN100C reworked PDIP's (U11 and U51) had many very early failures, all of which also exhibited possible trace cracks while their unreworked SnPb counterparts had no trace cracks and failed much later in the test.

### **QFN-20's**

The QFN's were resistant to failure under the conditions of this test. Only the QFN's in Position U47 had any failures (see Figure 35). Based on this limited data set, SAC305/Sn and SN100C/Sn underperformed the SnPb/SnPb controls and also underperformed SnPb/Sn and SAC305/SnPb.

### **TQFP-144's**

Most of the TQFP-144's had broken and/or missing leads at the end of the test (see Figure 36). Since most of the failures appeared to be due to broken leads, this might explain why many of the solder/finish combinations were equivalent in performance (see Figures 37 and 38). SAC305/Sn, SnPb/NiPdAu (on immersion Ag) and SN100C/Sn performed about as well as the SnPb/Sn control. SAC305/NiPdAu underperformed the SnPb/Sn control.

For this test, some Sn-plated TQFP-144 leads were dipped into either molten SnPb or SAC305 to evaluate the effectiveness of the hot solder dipping on tin whisker formation. The combination of SnPb/SnPb Dip was almost equivalent to the SnPb/Sn control in performance but the SAC305/SAC305 Dip performance was slightly inferior to that of the SnPb/Sn control (Figure 38).

### **TSOP-50's**

Figure 39 shows a crack typical of those found in the TSOP solder joints.

Some of the Alloy 42 TSOP's oriented parallel to the wedgelocks (U12, U16, U26, and U29) fell off during the testing. No TSOP's oriented perpendicular to the wedgelocks (U24, U25, U39, U40, U61, and U62) fell off during the testing. A similar orientation effect for TSOP's was also noted in the JCAA/JG-PP study [3]. The general failure mechanism for all of the TSOP's that fell off was for the leads to pull out of the solder. The effect of orientation upon which TSOP's fell off may have been due to the larger PWB radius of curvature change experienced by the foot of a TSOP lead when oriented perpendicular to the wedgelocks versus the smaller PWB radius of curvature change experienced by the foot of the lead when oriented parallel to the wedgelocks.

The orientation of the TSOP's may also have played a role in how well the solders performed and in their relative ranking. For example, with U16 (oriented parallel to the wedgelocks) the relative solder ranking was SnPb/SnPb > SN100C/SnBi > SAC305/SnBi. However, for U24 (oriented perpendicular to the wedgelocks) the relative solder ranking was SAC305/SnBi >= SnPb/SnPb > SN100C/SnBi (see Figures 40 and 41).

In general, when the TSOP was oriented parallel to the wedgelocks, SnPb outperformed SAC305 and when the TSOP was oriented perpendicular to the wedgelocks, SAC305 outperformed SnPb. The following combinations always underperformed SnPb/SnPb regardless of the orientation of the TSOP: SN100C/SnBi; SN100C/Sn; SAC305/SnPb; reworked SnPb/Sn (using either a SnPb or Pb-free thermal profile); reworked SnPb/SnPb; and reworked SAC305/SnBi.

When ranking the solders in Table 6, the orientation effect was ignored. If the solder/ finish combination performed better than the SnPb/SnPb control in one orientation and worse than the control in the other orientation, it was assigned the number “2” and the color “yellow”.

#### **Plated Through Holes (PTH's)**

No failures of the PTH nets were observed.

#### **SUMMARY**

The overall results of the vibration testing are summarized in Table 6. If a solder alloy/component finish combination performed as well or better than the SnPb control, it was assigned the number “1” and the color “green”. Solders that performed worse than the SnPb control were assigned a “2” and the color “yellow”. Solders that performed much worse than the SnPb control were assigned a “3” and the color “red”. The rankings in Table 6 are somewhat subjective due to the scatter in the data for some component types.

The pure lead-free systems of SAC305/SAC105 balls and SN100C/SAC105 balls (on CSP's), and SAC305/Sn and SN100C/Sn (on TQFP's) performed about as well as the SnPb controls.

The pure lead-free systems of SAC305/SAC405 balls and SN100C/SAC405 balls (on BGA's); SAC305/SAC305 and SN100C/SAC305 (on CLCC's); SN100C/Sn and SN100C/NiPdAu (on PDIP's); SAC305/Sn and SN100C/Sn (on QFN's); SAC305/NiPdAu and SAC305/SAC305 Dip (on TQFP's); and SAC305/Sn, SAC305/SnBi, SN100C/Sn, and SN100C/SnBi (on TSOP's) underperformed the SnPb controls.

Mixed technologies generally underperformed the SnPb controls. The exceptions were SnPb/SAC105 and reworked SnPb/SAC105 (on CSP's) and SAC305/SnPb (on QFN's).

Rework operations that yielded non-mixed technologies generally reduced the reliability of solder/finish combinations compared to their unreworked counterparts. The exceptions were the CSP's reworked with Flux Only/SnPb.

The lead-free PDIP's exhibited many early failures which contrasts with the results of the earlier JCAA/JG-PP study. There is evidence that these early failures were due to trace cracking. The trace cracking may have been promoted by substandard copper.

#### **CONCLUSIONS AND RECOMMENDATIONS**

The results of this study suggest that for many component types, the lead-free solders tested are not as reliable as eutectic SnPb solder with respect to vibration. Rework also had a negative effect on both SnPb and lead-free solders with respect to vibration.

Each aerospace/military program will have to do their own qualification tests to determine if lead-free solders are appropriate for use in an electronic design on a specific platform. The development of validated models for predicting how long a specific design will survive in a specific vibration environment would be of great benefit.

For severe vibration environments, the use of lead-free solders may require the use of stiffeners, bumpers, or vibration isolators to reduce PWA flexure and reduce solder joint strains to acceptable levels.

#### **ACKNOWLEDGEMENTS**

Thanks to Tom Kowalski for running the electrodynamic shaker and collecting accelerometer and strain gage data. Thanks to Don Powers for conducting the laser vibrometer modal analysis and collecting laser data for the full field strain calculations. A special thanks to ITB, Inc. for funding testing of the vibration test vehicles.

#### **REFERENCES**

- [1] NASA-DoD Lead-Free Electronics Project Plan, August 2009.
- [2] Woodrow, T.A., “NASA-DoD Lead-Free Electronics Project: Vibration Test”, Boeing Electronics Materials and Processes Report-603, June 30, 2010 (this document can be found at [http://www.acqp2.nasa.gov/NASA\\_DODLeadFreeElectronics\\_Proj2.html](http://www.acqp2.nasa.gov/NASA_DODLeadFreeElectronics_Proj2.html)).
- [3] Woodrow, T.A., “JCAA/JG-PP Lead-Free Solder Project: Vibration Test”, Boeing Electronics Materials and Processes Report-582, Revision A, January 9, 2006 (this document can be found at [http://www.acqp2.nasa.gov/LeadFreeSolderTestingForHighReliability\\_Proj1.html](http://www.acqp2.nasa.gov/LeadFreeSolderTestingForHighReliability_Proj1.html)).

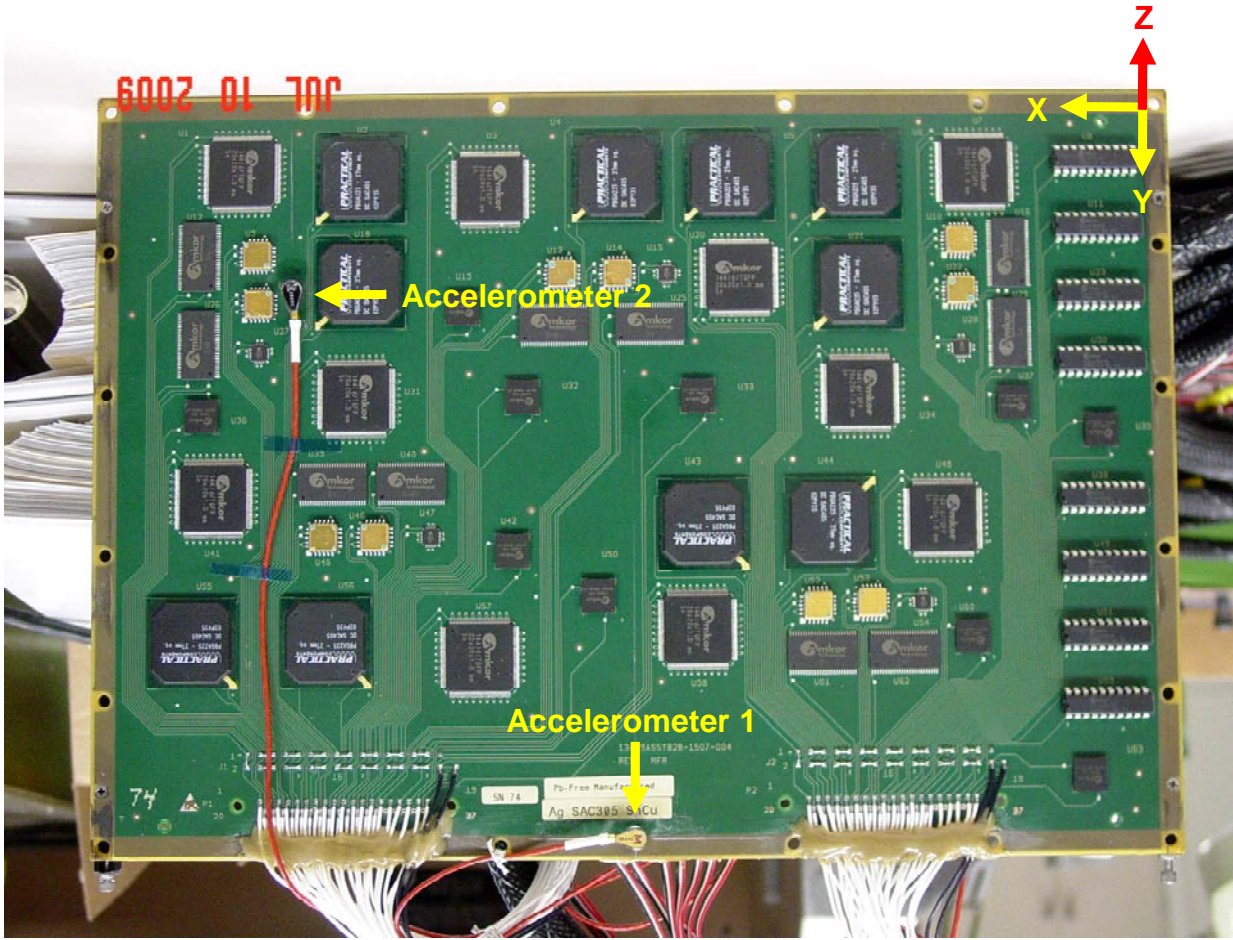


Figure 1. NASA-DOD Test Vehicle

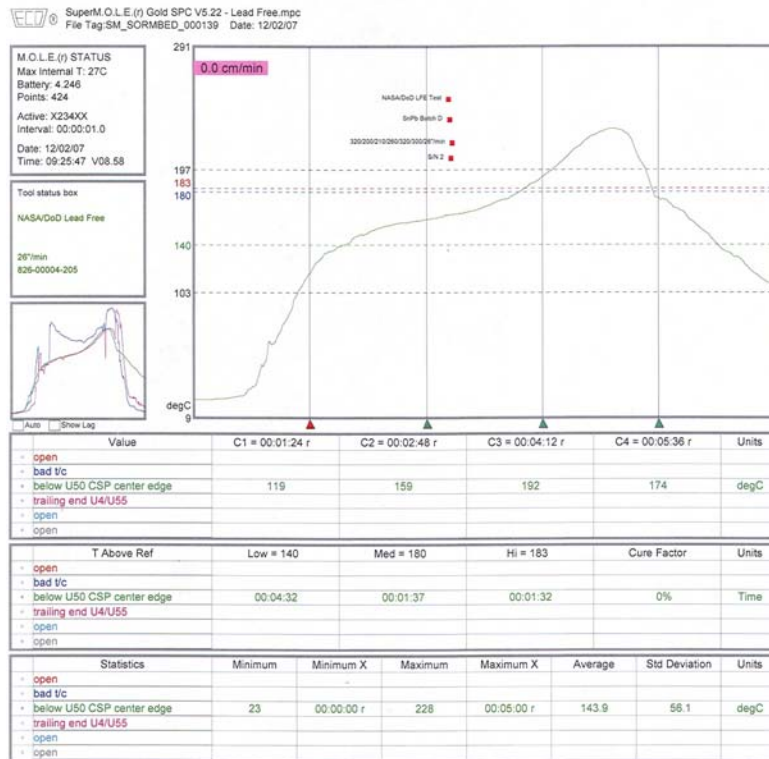


Figure 2. Reflow Profile for SnPb Solder Paste (Source: BAE Systems)

**Table 1.** Assembly Matrix for “Manufactured” Vibration Test Vehicles

		SnPb "Manufactured" Test Vehicles			Pb-Free "Manufactured" Test Vehicles (SAC305 Paste)			Pb-Free "Manufactured" Test Vehicles (SN100C Paste)		
		Test Vehicles 15, 16, 17, 18, 19			Test Vehicles 36, 40, 74, 76, 78, 96 (on ENIG)			Test Vehicles 111, 112, 113, 114, 115		
RefDes	Component	Component Finish	Reflow Solder Alloy	Wave Solder Alloy	Component Finish	Reflow Solder Alloy	Wave Solder Alloy	Component Finish	Reflow Solder Alloy	Wave Solder Alloy
U18	BGA-225	SnPb	SnPb		SAC405	SAC305		SAC405	SN100C	
U43	BGA-225	SnPb	SnPb		SAC405	SAC305		SAC405	SN100C	
U04	BGA-225	SnPb	SnPb		SAC405	SAC305		SAC405	SN100C	
U06	BGA-225	SnPb	SnPb		SAC405	SAC305		SAC405	SN100C	
U55	BGA-225	SnPb	SnPb		SAC405	SAC305		SAC405	SN100C	
U02	BGA-225	SnPb	SnPb		SAC405	SAC305		SAC405	SN100C	
U05	BGA-225	SnPb	SnPb		SAC405	SAC305		SAC405	SN100C	
U21	BGA-225	SnPb	SnPb		SAC405	SAC305		SAC405	SN100C	
U44	BGA-225	SnPb	SnPb		SAC405	SAC305		SAC405	SN100C	
U56	BGA-225	SnPb	SnPb		SAC405	SAC305		SAC405	SN100C	
U09	CLCC-20	SnPb	SnPb		SAC305	SAC305		SAC305	SN100C	
U13	CLCC-20	SnPb	SnPb		SAC305	SAC305		SAC305	SN100C	
U22	CLCC-20	SnPb	SnPb		SAC305	SAC305		SAC305	SN100C	
U46	CLCC-20	SnPb	SnPb		SAC305	SAC305		SAC305	SN100C	
U53	CLCC-20	SnPb	SnPb		SAC305	SAC305		SAC305	SN100C	
U10	CLCC-20	SnPb	SnPb		SAC305	SAC305		SAC305	SN100C	
U14	CLCC-20	SnPb	SnPb		SAC305	SAC305		SAC305	SN100C	
U17	CLCC-20	SnPb	SnPb		SAC305	SAC305		SAC305	SN100C	
U45	CLCC-20	SnPb	SnPb		SAC305	SAC305		SAC305	SN100C	
U52	CLCC-20	SnPb	SnPb		SAC305	SAC305		SAC305	SN100C	
U32	CSP-100	SnPb	SnPb		SAC105	SAC305		SAC105	SN100C	
U33	CSP-100	SnPb	SnPb		SAC105	SAC305		SAC105	SN100C	
U35	CSP-100	SnPb	SnPb		SAC105	SAC305		SAC105	SN100C	
U50	CSP-100	SnPb	SnPb		SAC105	SAC305		SAC105	SN100C	
U63	CSP-100	SnPb	SnPb		SAC105	SAC305		SAC105	SN100C	
U19	CSP-100	SnPb	SnPb		SAC105	SAC305		SAC105	SN100C	
U36	CSP-100	SnPb	SnPb		SAC105	SAC305		SAC105	SN100C	
U37	CSP-100	SnPb	SnPb		SAC105	SAC305		SAC105	SN100C	
U42	CSP-100	SnPb	SnPb		SAC105	SAC305		SAC105	SN100C	
U60	CSP-100	SnPb	SnPb		SAC105	SAC305		SAC105	SN100C	
U08	PDIP-20	SnPb		SnPb	See Reference 2		SN100C	NiPdAu		SN100C
U23	PDIP-20	SnPb		SnPb	See Reference 2		SN100C	NiPdAu		SN100C
U49	PDIP-20	SnPb		SnPb	See Reference 2		SN100C	NiPdAu		SN100C
U59	PDIP-20	SnPb		SnPb	See Reference 2		SN100C	Sn		SN100C
U30	PDIP-20	SnPb		SnPb	See Reference 2		SN100C	Sn		SN100C
U38	PDIP-20	SnPb		SnPb	See Reference 2		SN100C	Sn		SN100C
U11	PDIP-20	SnPb		SnPb	See Reference 2		SN100C	Sn		SN100C
U51	PDIP-20	SnPb		SnPb	See Reference 2		SN100C	Sn		SN100C
U15	QFN-20	SnPb	SnPb		Matte Sn	SAC305		Matte Sn	SN100C	
U27	QFN-20	SnPb	SnPb		Matte Sn	SAC305		Matte Sn	SN100C	
U28	QFN-20	SnPb	SnPb		Matte Sn	SAC305		Matte Sn	SN100C	
U47	QFN-20	SnPb	SnPb		Matte Sn	SAC305		Matte Sn	SN100C	
U54	QFN-20	SnPb	SnPb		Matte Sn	SAC305		Matte Sn	SN100C	
U01	TQFP-144	Matte Sn	SnPb		Matte Sn	SAC305		Matte Sn	SN100C	
U07	TQFP-144	Matte Sn	SnPb		Matte Sn	SAC305		Matte Sn	SN100C	
U20	TQFP-144	Matte Sn	SnPb		Matte Sn	SAC305		Matte Sn	SN100C	
U41	TQFP-144	Matte Sn	SnPb		Matte Sn	SAC305		Matte Sn	SN100C	
U58	TQFP-144	Matte Sn	SnPb		Matte Sn	SAC305		Matte Sn	SN100C	
U03	TQFP-144	Matte Sn	SnPb		Matte Sn	SAC305		Matte Sn	SN100C	
U31	TQFP-144	Matte Sn	SnPb		Matte Sn	SAC305		Matte Sn	SN100C	
U34	TQFP-144	Matte Sn	SnPb		Matte Sn	SAC305		Matte Sn	SN100C	
U48	TQFP-144	Matte Sn	SnPb		Matte Sn	SAC305		Matte Sn	SN100C	
U57	TQFP-144	Matte Sn	SnPb		Matte Sn	SAC305		Matte Sn	SN100C	
U12	TSOP-50	SnPb	SnPb		Sn	SAC305		Sn	SN100C	
U25	TSOP-50	SnPb	SnPb		Sn	SAC305		Sn	SN100C	
U29	TSOP-50	SnPb	SnPb		Sn	SAC305		Sn	SN100C	
U39	TSOP-50	SnPb	SnPb		Sn	SAC305		Sn	SN100C	
U61	TSOP-50	SnPb	SnPb		Sn	SAC305		Sn	SN100C	
U16	TSOP-50	SnPb	SnPb		SnBi	SAC305		SnBi	SN100C	
U24	TSOP-50	SnPb	SnPb		SnBi	SAC305		SnBi	SN100C	
U26	TSOP-50	SnPb	SnPb		SnBi	SAC305		SnBi	SN100C	
U40	TSOP-50	SnPb	SnPb		SnBi	SAC305		SnBi	SN100C	
U62	TSOP-50	SnPb	SnPb		SnBi	SAC305		SnBi	SN100C	

**Table 2.** Assembly Matrix for “Rework” Vibration Test Vehicles

		SnPb "Rework" Test Vehicles					Pb-Free "Rework" Test Vehicles				
		Test Vehicles 134, 135, 136, 137, 138, 157 (on ENIG)					Test Vehicles 174, 175, 176, 177, 178				
RefDes	Component	Original Component Finish	Reflow Solder Alloy	Wave Solder Alloy	New Component Finish	Rework Solder	Component Finish	Reflow Solder Alloy	Wave Solder Alloy	New Component Finish	Rework Solder
U04	BGA-225	SAC405	SnPb				SnPb	SAC305			
U55	BGA-225	SAC405	SnPb				SnPb	SAC305			
U05	BGA-225	SAC405	SnPb				SnPb	SAC305			
U44	BGA-225	SAC405	SnPb				SnPb	SAC305			
U18	BGA-225	SnPb	SnPb		SAC405	SnPb	SAC405	SAC305		SAC405	SnPb
U43	BGA-225	SnPb	SnPb		SAC405	SnPb	SAC405	SAC305		SAC405	SnPb
U06	BGA-225	SnPb	SnPb		SAC405	SnPb	SAC405	SAC305		SAC405	SnPb
U02	BGA-225	SnPb	SnPb		SnPb	Flux Only	SAC405	SAC305		SAC405	Flux Only
U21	BGA-225	SnPb	SnPb		SnPb	Flux Only	SAC405	SAC305		SAC405	Flux Only
U56	BGA-225	SnPb	SnPb		SnPb	Flux Only	SAC405	SAC305		SAC405	Flux Only
U09	CLCC-20	SAC305	SnPb				SnPb	SAC305			
U10	CLCC-20	SAC305	SnPb				SnPb	SAC305			
U13	CLCC-20	SAC305	SnPb				SnPb	SAC305			
U14	CLCC-20	SAC305	SnPb				SnPb	SAC305			
U17	CLCC-20	SAC305	SnPb				SnPb	SAC305			
U22	CLCC-20	SAC305	SnPb				SnPb	SAC305			
U45	CLCC-20	SAC305	SnPb				SnPb	SAC305			
U46	CLCC-20	SAC305	SnPb				SnPb	SAC305			
U52	CLCC-20	SAC305	SnPb				SnPb	SAC305			
U53	CLCC-20	SAC305	SnPb				SnPb	SAC305			
U32	CSP-100	SAC105	SnPb				SnPb	SAC305			
U35	CSP-100	SAC105	SnPb				SnPb	SAC305			
U63	CSP-100	SAC105	SnPb				SnPb	SAC305			
U36	CSP-100	SAC105	SnPb				SAC105	SAC305			
U50	CSP-100	SnPb	SnPb		SnPb	Flux Only	SAC105	SAC305		SAC105	Flux Only
U19	CSP-100	SnPb	SnPb		SnPb	Flux Only	SAC105	SAC305		SAC105	Flux Only
U37	CSP-100	SnPb	SnPb		SnPb	Flux Only	SAC105	SAC305		SAC105	Flux Only
U33	CSP-100	SnPb	SnPb		SAC105	SnPb	SAC105	SAC305		SAC105	SnPb
U42	CSP-100	SnPb	SnPb		SAC105	SnPb	SAC105	SAC305		SAC105	SnPb
U60	CSP-100	SnPb	SnPb		SAC105	SnPb	SAC105	SAC305		SAC105	SnPb
U08	PDIP-20	NiPdAu		SnPb			Sn		SN100C		
U23	PDIP-20	NiPdAu		SnPb			Sn		SN100C		
U49	PDIP-20	NiPdAu		SnPb			Sn		SN100C		
U59	PDIP-20	Sn		SnPb			Sn		SN100C		
U30	PDIP-20	Sn		SnPb			Sn		SN100C		
U38	PDIP-20	Sn		SnPb			Sn		SN100C		
U11	PDIP-20	SnPb		SnPb	Sn	SnPb	Sn		SN100C	Sn	SN100C
U51	PDIP-20	SnPb		SnPb	Sn	SnPb	Sn		SN100C	Sn	SN100C
U15	QFN-20	Matte Sn	SnPb				SnPb	SAC305			
U27	QFN-20	Matte Sn	SnPb				SnPb	SAC305			
U28	QFN-20	Matte Sn	SnPb				SnPb	SAC305			
U47	QFN-20	Matte Sn	SnPb				SnPb	SAC305			
U54	QFN-20	Matte Sn	SnPb				SnPb	SAC305			
U03	TQFP-144	NiPdAu	SnPb				NiPdAu	SAC305			
U31	TQFP-144	NiPdAu	SnPb				NiPdAu	SAC305			
U34	TQFP-144	NiPdAu	SnPb				NiPdAu	SAC305			
U48	TQFP-144	NiPdAu	SnPb				NiPdAu	SAC305			
U57	TQFP-144	NiPdAu	SnPb				NiPdAu	SAC305			
U01	TQFP-144	SnPb Dip	SnPb				SAC 305 Dip	SAC305			
U07	TQFP-144	SnPb Dip	SnPb				SAC 305 Dip	SAC305			
U20	TQFP-144	SnPb Dip	SnPb				SAC 305 Dip	SAC305			
U41	TQFP-144	SnPb Dip	SnPb				SAC 305 Dip	SAC305			
U58	TQFP-144	SnPb Dip	SnPb				SAC 305 Dip	SAC305			
U29	TSOP-50	Sn	SnPb				SnBi	SAC305			
U39	TSOP-50	Sn	SnPb				SnBi	SAC305			
U61	TSOP-50	Sn	SnPb				SnBi	SAC305			
U16	TSOP-50	SnBi	SnPb				SnPb	SAC305			
U40	TSOP-50	SnBi	SnPb				SnPb	SAC305			
U62	TSOP-50	SnBi	SnPb				SnPb	SAC305			
U12	TSOP-50	SnPb	SnPb		SnPb	SnPb	Sn	SAC305		Sn	SnPb
U25	TSOP-50	SnPb	SnPb		SnPb	SnPb	Sn	SAC305		Sn	SnPb
U24	TSOP-50	SnPb	SnPb		Sn	SnPb	SnBi	SAC305		SnBi	SAC305
U26	TSOP-50	SnPb	SnPb		Sn	SnPb	SnBi	SAC305		SnBi	SAC305

Mixed SnPb/Pb-Free  
 Sn Plating Dipped for Whisker Mitigation

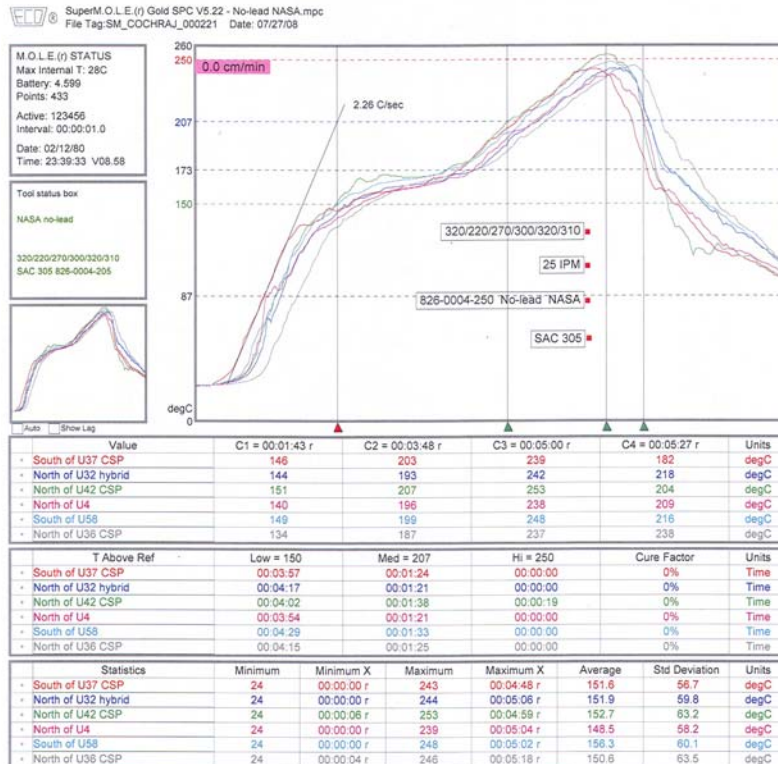


**Figure 3.** Reflow Profile for SAC305 and SN100C Solder Pastes  
(Source: BAE Systems)

**Table 3.** Chemical Analysis of Solder Joints Contaminated with Pb (by ICP Spectroscopy)

Component	Ref. Des.	Test Vehicle ID	Reworked?	Component Finish	Board Finish	Solder	%Ag	%Cu	%Pb	%Sn	%Bi	%Au
BGA-225	U04	149	No	SAC405	Ag	Sn37Pb	3.46	0.94	3.77	91.71	0.00	0.13
BGA-225	U04	193	No	Sn37Pb	Ag	SAC305	0.31	0.26	33.91	65.44	0.00	0.08
BGA-225	U43	193	Yes	SAC405	Residual SAC	Sn37Pb	3.13	3.18**	5.52	88.07	0.00	0.10
CLCC-20	U09	149	No	SAC305	Ag	Sn37Pb	1.35	0.49	24.68	73.48	0.00	0.00
CLCC-20	U09	193	No	Sn37Pb	Ag	SAC305	1.92	0.39	16.46	81.19	0.04	0.00
CSP-100*	U33	149	Yes	SAC105	Residual Sn37Pb	Sn37Pb	0.90	0.73	1.81	96.23	0.00	0.33
CSP-100*	U33	193	Yes	SAC105	Residual SAC	Sn37Pb	0.83	0.63	4.43	93.82	0.00	0.29
QFN-20	U15	193	No	SnPb	Ag	SAC305	3.39	0.85	0.93	94.83	0.00	0.00
TSOP-50	U16	149	No	SnBi	Ag	Sn37Pb	0.44	2.68**	35.73	61.06	0.09	0.00
TSOP-50	U16	193	No	SnPb	Ag	SAC305	3.53	6.10**	1.51	88.86	0.00	0.00

\*PWB Cu pads had to be cut from the CSP balls. This operation also removed that end of each ball.

\*\* Copper may have been removed from the PWB pads when the solder joints were cut from the test vehicle.



**Figure 4.** Test Vehicles in Fixture

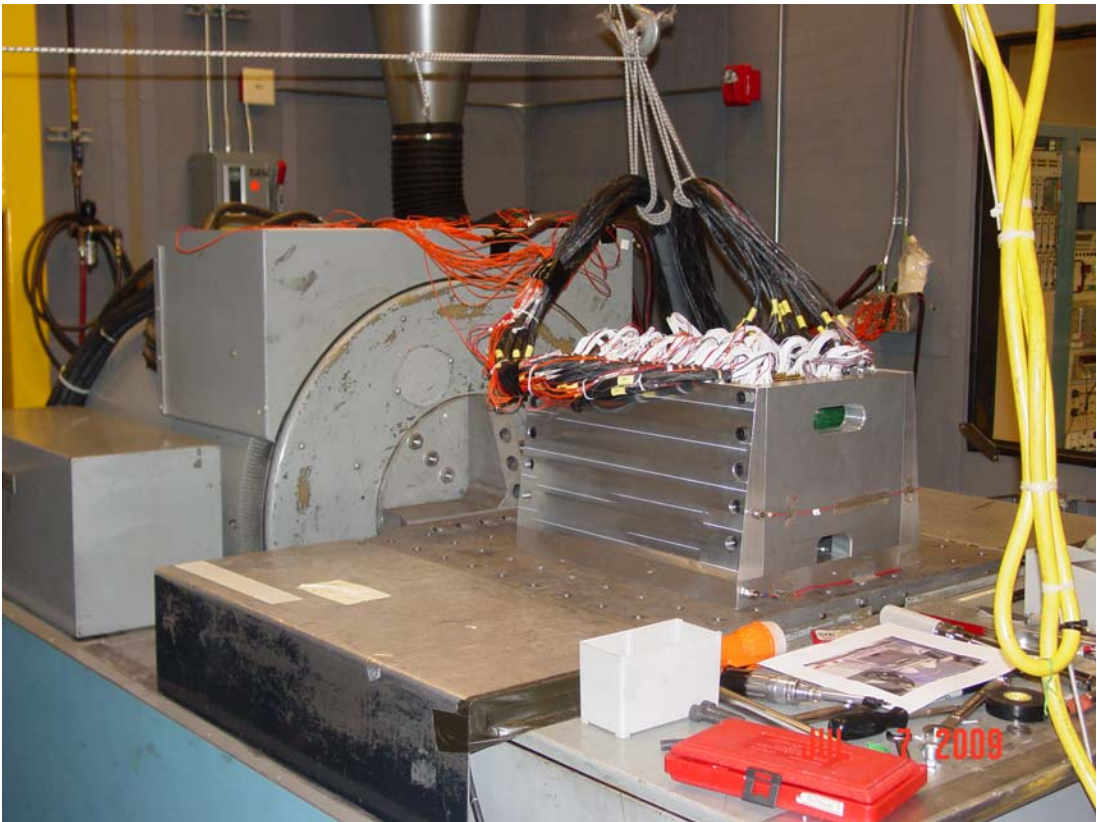


**Figure 5.** Test Vehicles in Fixture Mounted on the Electrodynamic Shaker

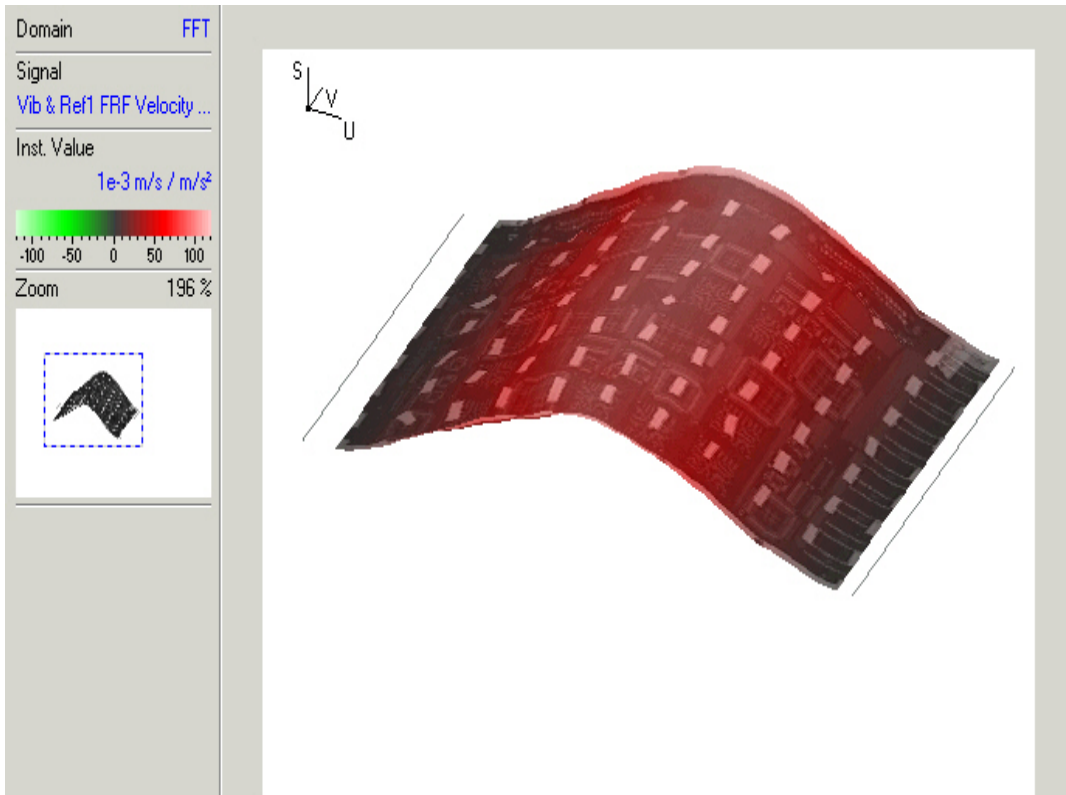


**Figure 6.** Mode Shape at 65 Hz

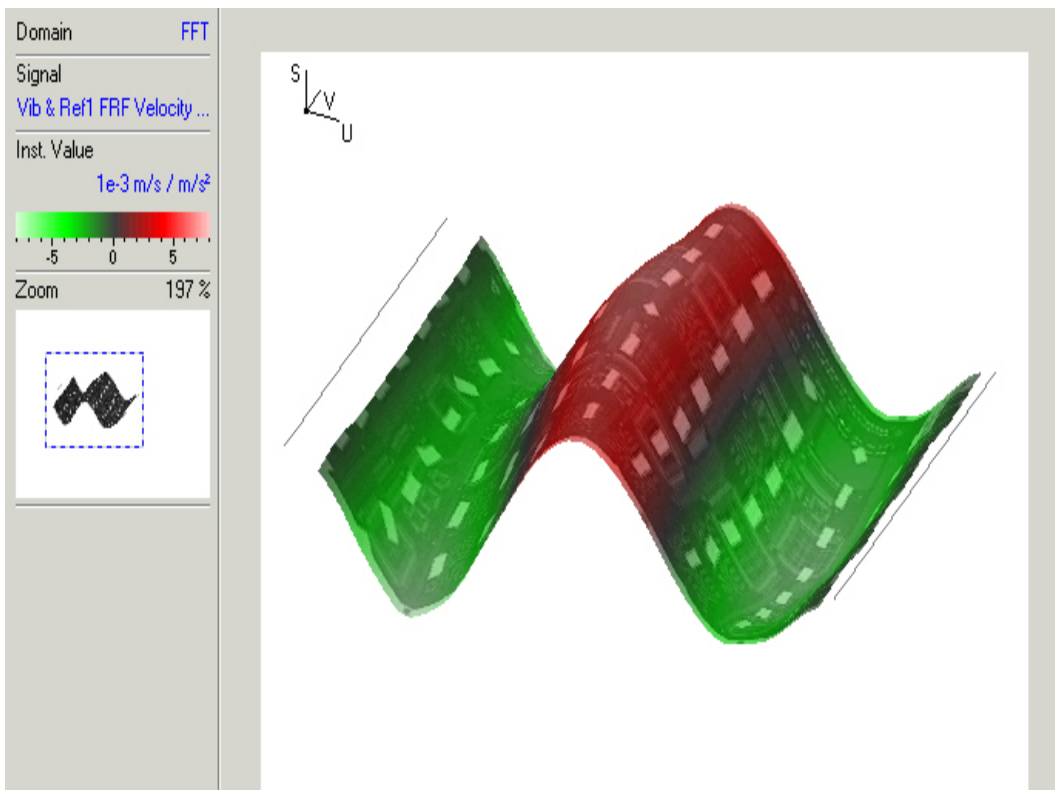


**Figure 7.** Mode Shape at 390 Hz

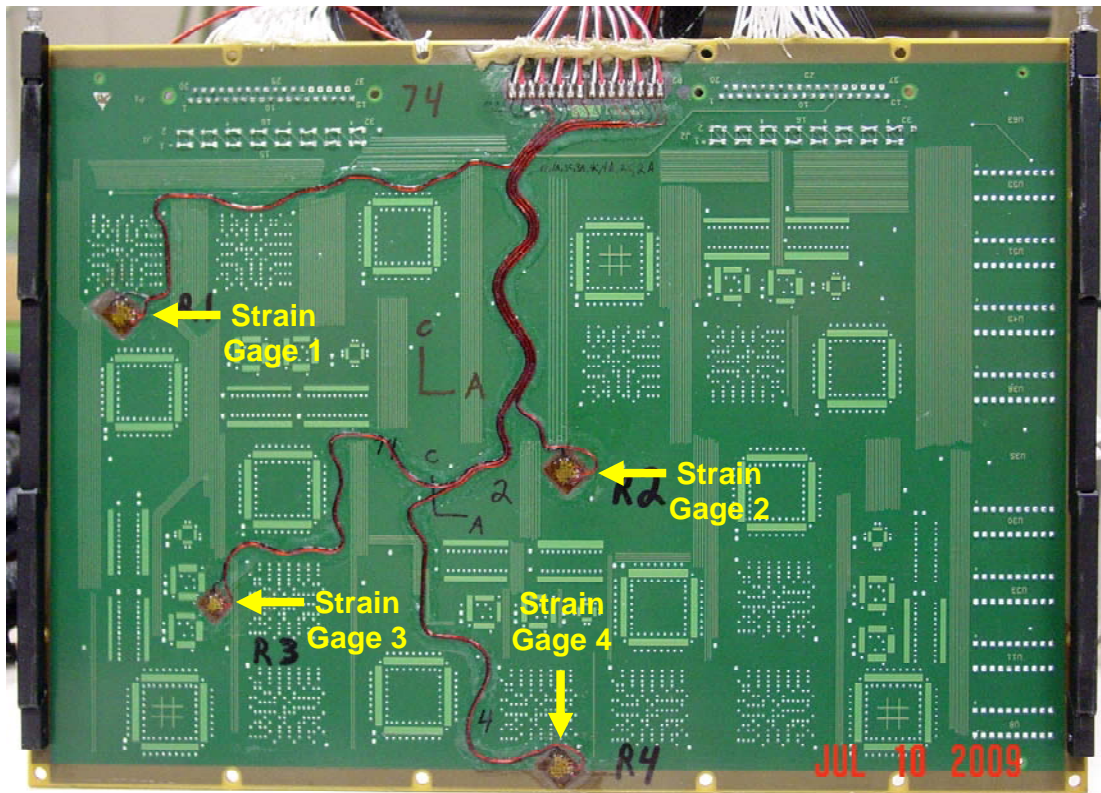


**Figure 8.** Strain Gage Placement on Test Vehicle 74

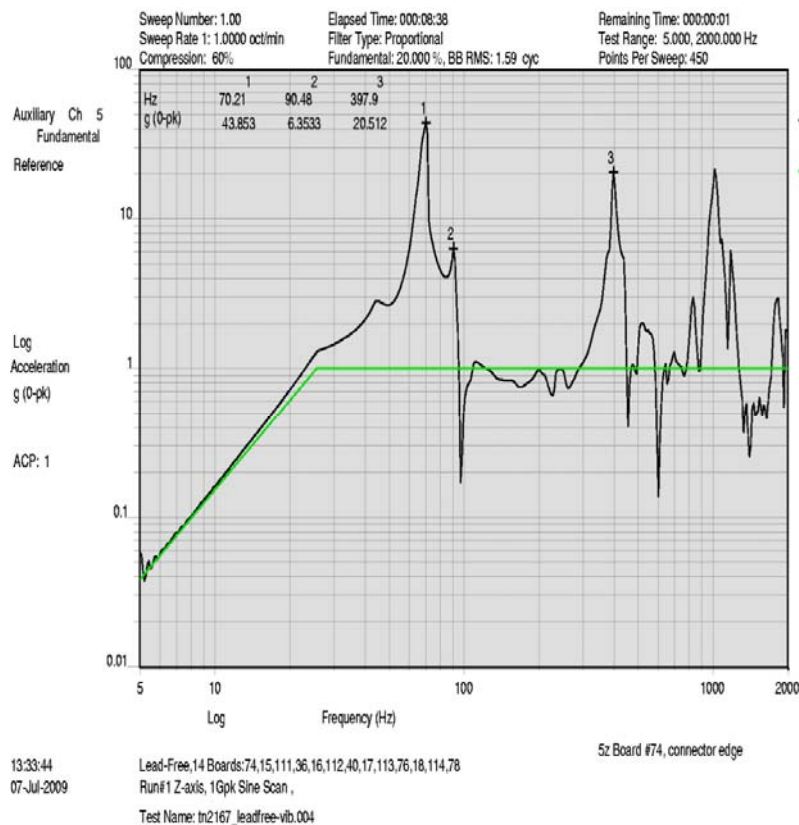


**Figure 9.** Transmissibilities at Each Major Resonant Frequency Measured During a 1G Sine Sweep (Accelerometer 1, Test Vehicle 74)

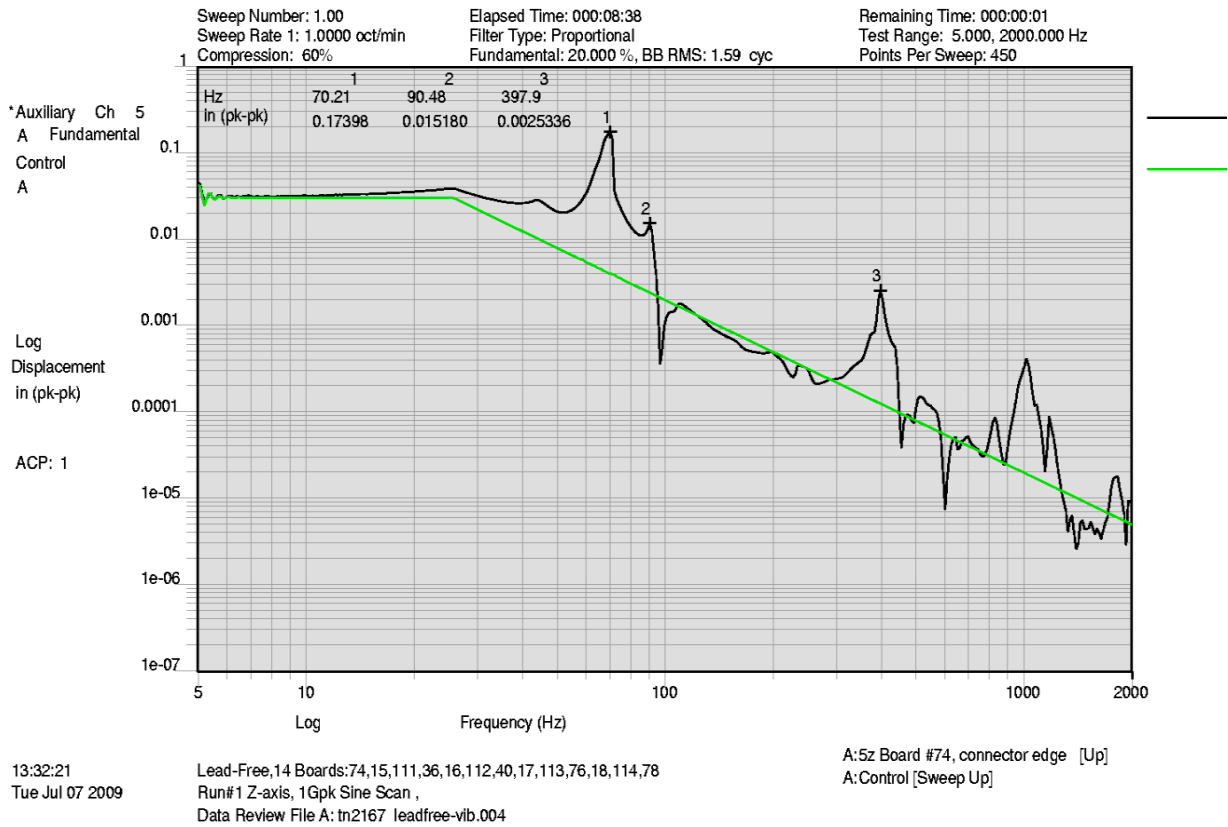


**Figure 10.** Displacements Measured During a 1G Sine Sweep (Accelerometer 1, Test Vehicle 74)

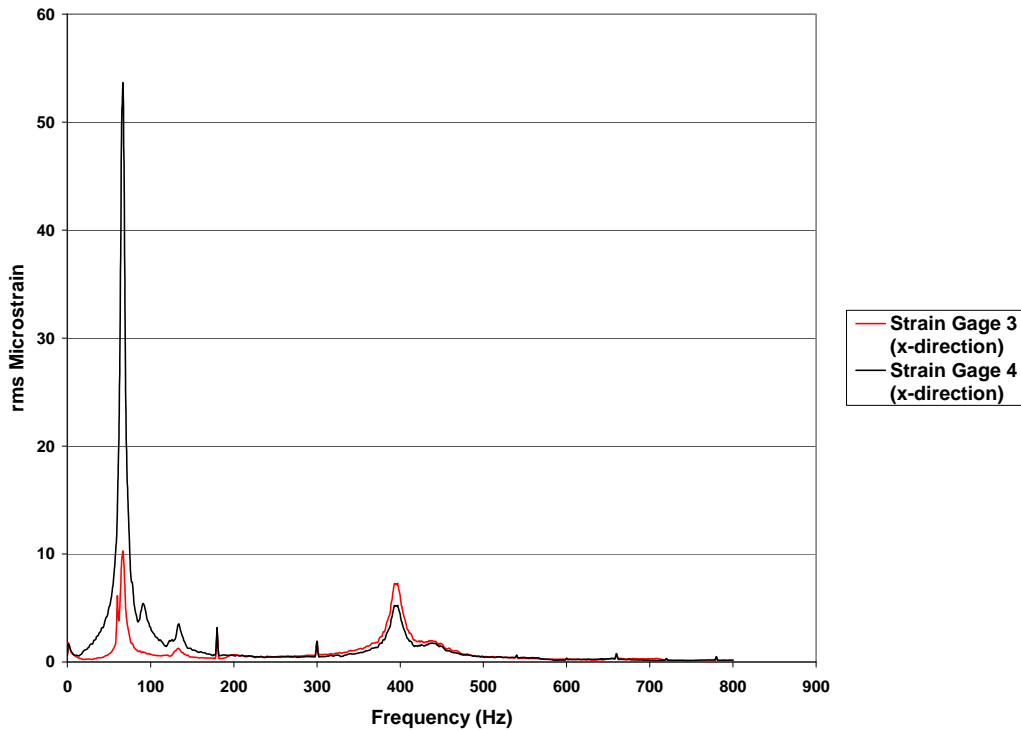


**Figure 11.** Microstrain vs. Frequency Measured during 8.0 Grms Test Level (Strain Gages 3 and 4, Test Vehicle 74)

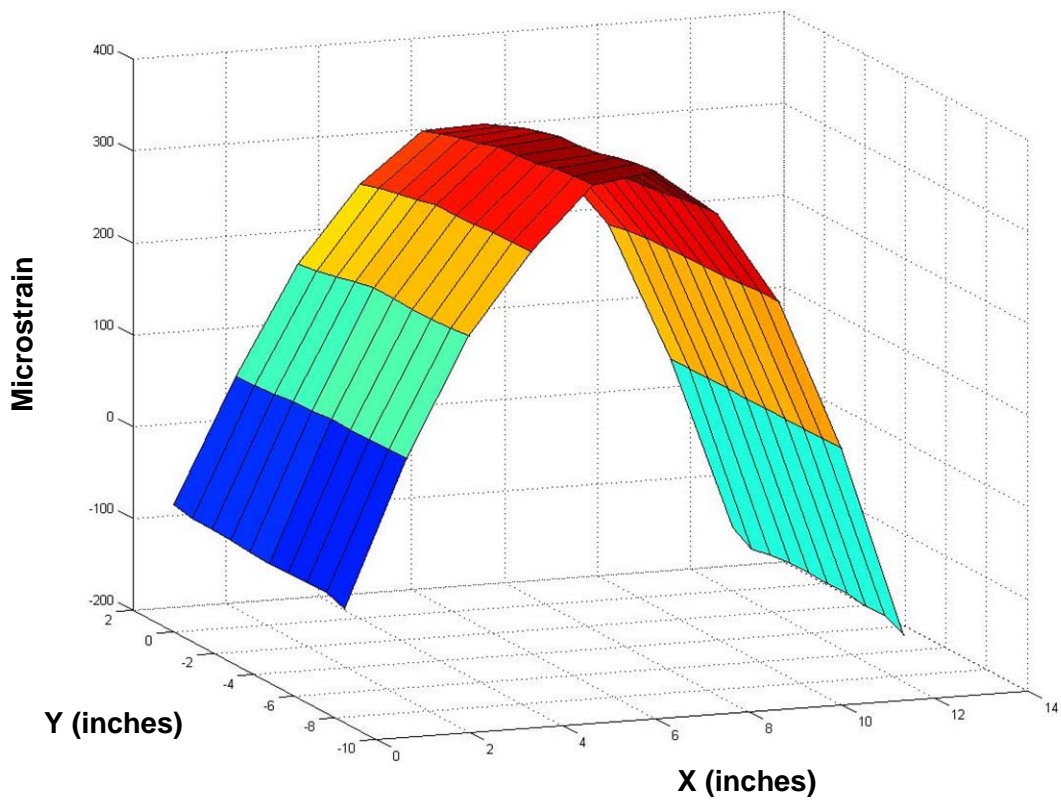


**Figure 12.** Full Field Peak Strains at 65 Hz (1G Sine Dwell, Test Vehicle 74)

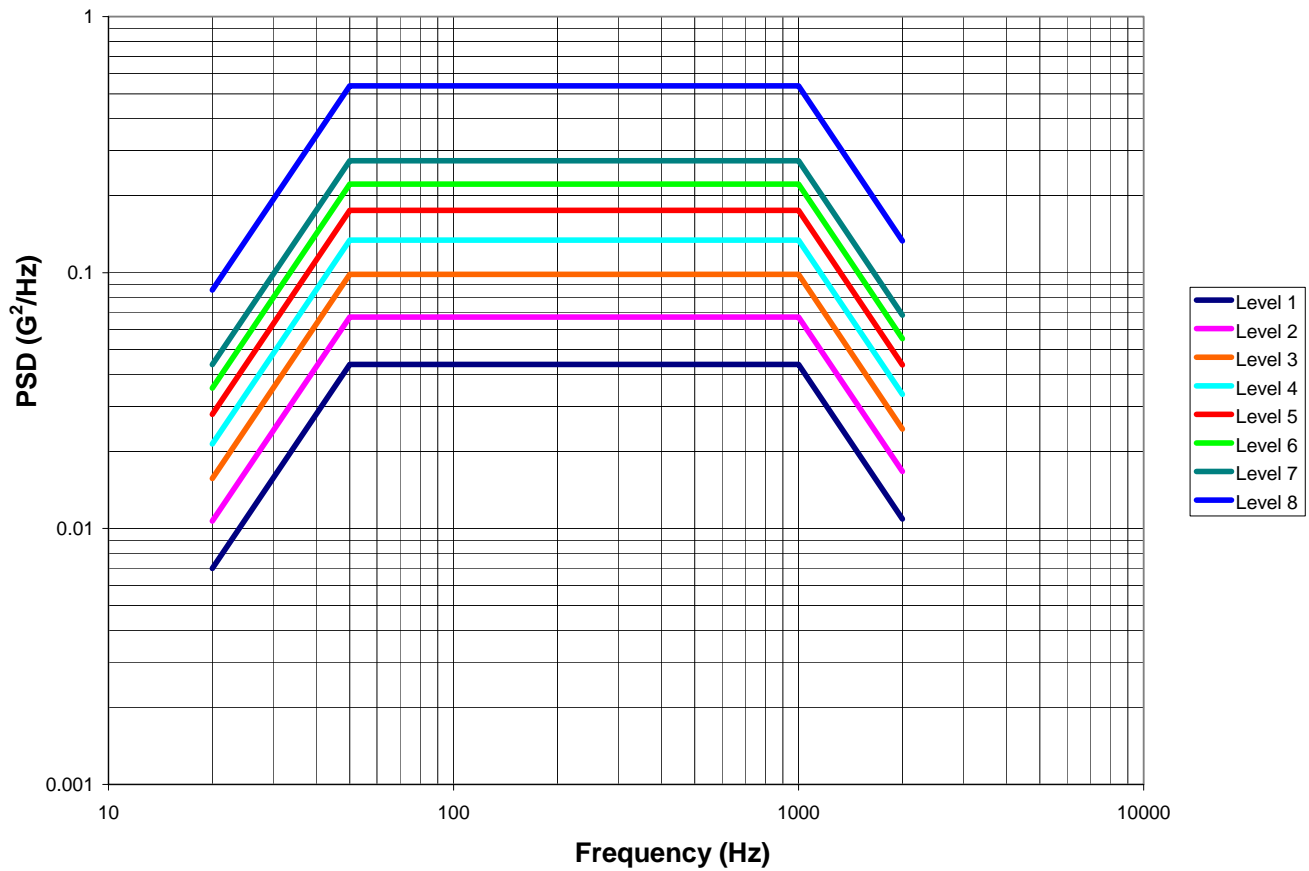


**Figure 13.** Vibration PSD's for Step Stress Test

**Table 4.** Vibration Test Levels

Level 1	Level 2	Level 3
20 Hz @ 0.00698 G <sup>2</sup> /Hz	20 Hz @ 0.0107 G <sup>2</sup> /Hz	20 Hz @ 0.0157 G <sup>2</sup> /Hz
20 - 50 Hz @ +6.0 dB/octave	20 - 50 Hz @ +6.0 dB/octave	20 - 50 Hz @ +6.0 dB/octave
50 - 1000 Hz @ 0.0438 G <sup>2</sup> /Hz	50 - 1000 Hz @ 0.067 G <sup>2</sup> /Hz	50 - 1000 Hz @ 0.0984 G <sup>2</sup> /Hz
1000 - 2000 Hz @ -6.0 dB/octave	1000 - 2000 Hz @ -6.0 dB/octave	1000 - 2000 Hz @ -6.0 dB/octave
2000 Hz @ 0.0109 G <sup>2</sup> /Hz	2000 Hz @ 0.0167 G <sup>2</sup> /Hz	2000 Hz @ 0.0245 G <sup>2</sup> /Hz
<b>Composite = 8.0 G<sub>rms</sub></b>	<b>Composite = 9.9 G<sub>rms</sub></b>	<b>Composite = 12.0 G<sub>rms</sub></b>

Level 4	Level 5	Level 6
20 Hz @ 0.0214 G <sup>2</sup> /Hz	20 Hz @ 0.0279 G <sup>2</sup> /Hz	20 Hz @ 0.0354 G <sup>2</sup> /Hz
20 - 50 Hz @ +6.0 dB/octave	20 - 50 Hz @ +6.0 dB/octave	20 - 50 Hz @ +6.0 dB/octave
50 - 1000 Hz @ 0.134 G <sup>2</sup> /Hz	50 - 1000 Hz @ 0.175 G <sup>2</sup> /Hz	50 - 1000 Hz @ 0.2215 G <sup>2</sup> /Hz
1000 - 2000 Hz @ -6.0 dB/octave	1000 - 2000 Hz @ -6.0 dB/octave	1000 - 2000 Hz @ -6.0 dB/octave
2000 Hz @ 0.0334 G <sup>2</sup> /Hz	2000 Hz @ 0.0436 G <sup>2</sup> /Hz	2000 Hz @ 0.0552 G <sup>2</sup> /Hz
<b>Composite = 14.0 G<sub>rms</sub></b>	<b>Composite = 16.0 G<sub>rms</sub></b>	<b>Composite = 18.0 G<sub>rms</sub></b>

Level 7	Level 8
20 Hz @ 0.0437 G <sup>2</sup> /Hz	20 Hz @ 0.0855 G <sup>2</sup> /Hz
20 - 50 Hz @ +6.0 dB/octave	20 - 50 Hz @ +6.0 dB/octave
50 - 1000 Hz @ 0.2734 G <sup>2</sup> /Hz	50 - 1000 Hz @ 0.5360 G <sup>2</sup> /Hz
1000 - 2000 Hz @ -6.0 dB/octave	1000 - 2000 Hz @ -6.0 dB/octave
2000 Hz @ 0.0682 G <sup>2</sup> /Hz	2000 Hz @ 0.1330 G <sup>2</sup> /Hz
<b>Composite = 20.0 G<sub>rms</sub></b>	<b>Composite = 28.0 G<sub>rms</sub></b>

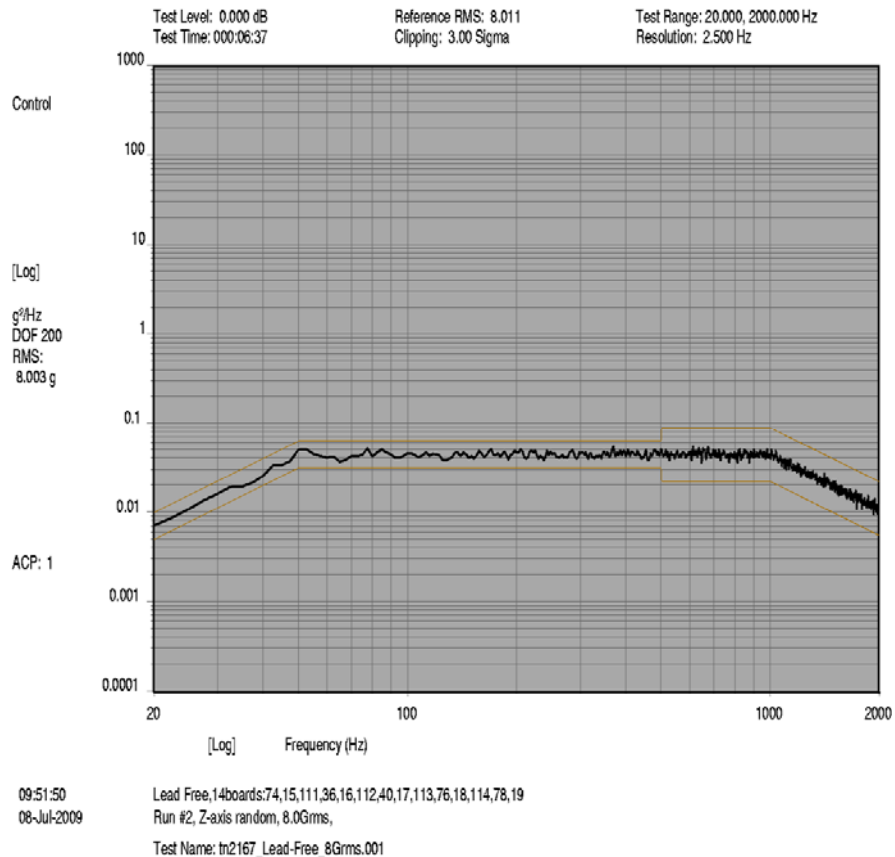


**Figure 14.** 8.0 Grms Input (Z-axis)

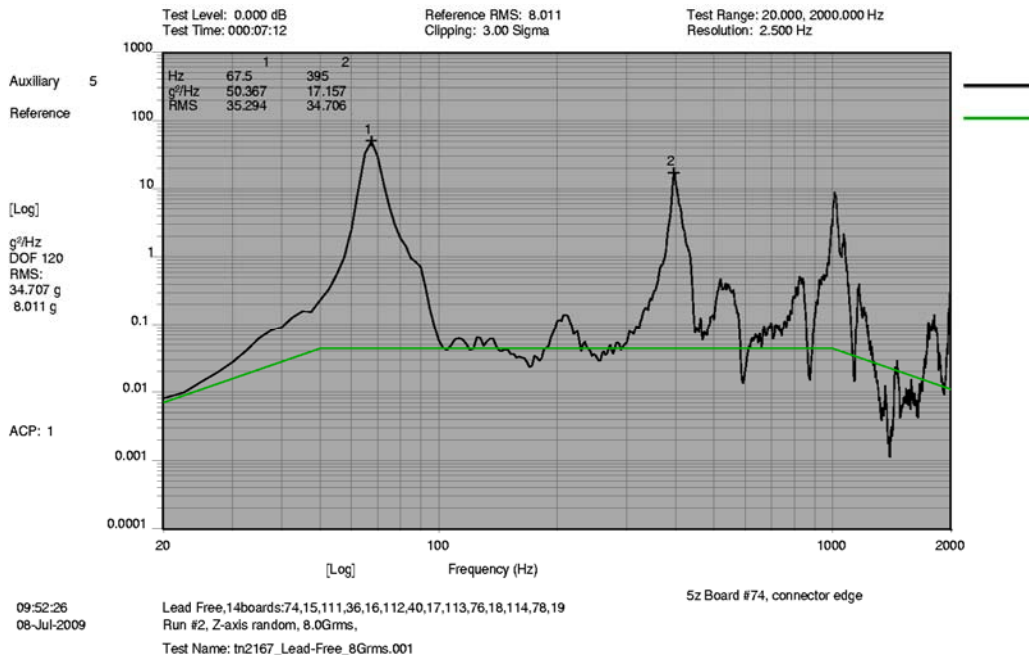


**Figure 15.** Test Vehicle Response (8.0 Grms, Z-axis, Accelerometer 1, Test Vehicle 74)

**Table 5.** % of Components Failed (Includes Mixed Solders)

<b>% of Components Failed During Vibration Testing</b>					
<b>Component</b>	<b>"Manufactured" Test Vehicles</b>			<b>"Rework" Test Vehicles</b>	
	<b>SnPb Paste</b>	<b>SAC305 Paste</b>	<b>SN100C Paste</b>	<b>SnPb Paste</b>	<b>Pb-Free Paste</b>
BGA-225	84	98	100	100	100
CLCC-20	32	43	90	35	68
CSP-100	62	73	70	62	80
PDIP-20	98	92	100	88	96
QFN-20	0	21	20	8	10
TQFP-144	60	63	64	70	70
TSOP-50	62	73	86	77	80

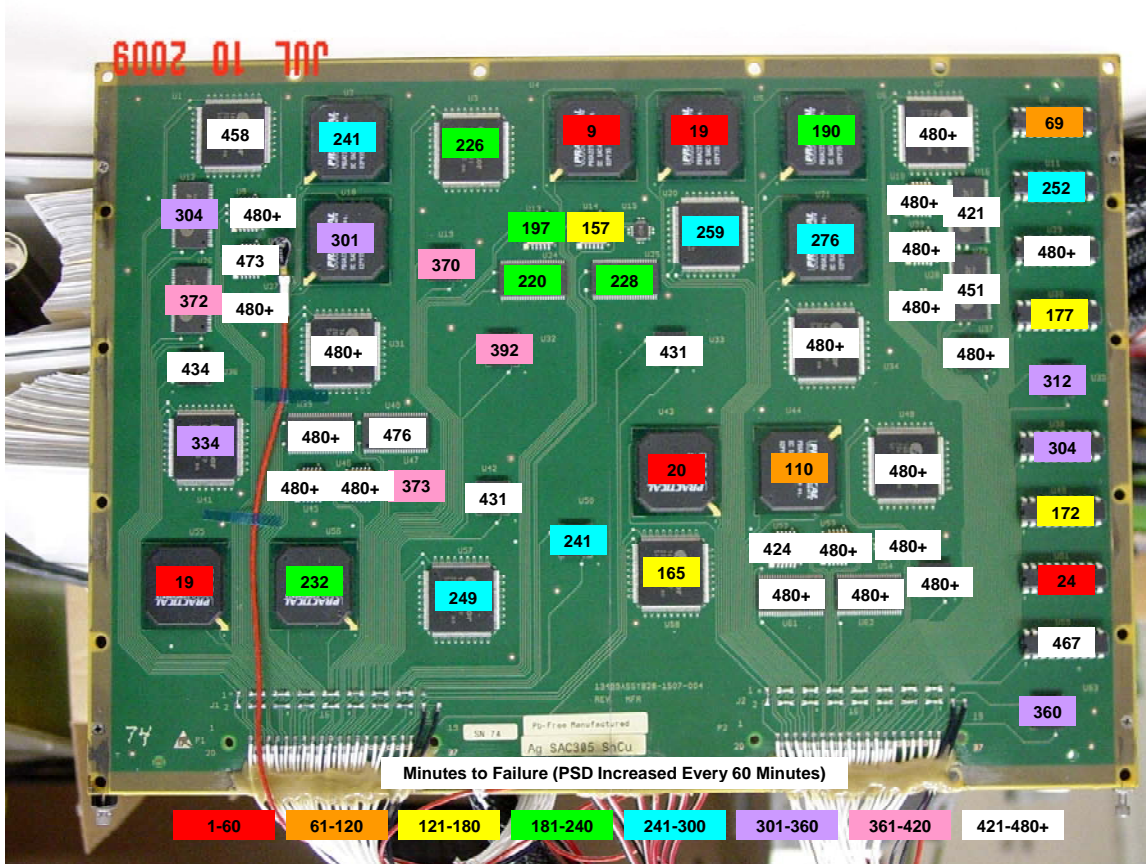


Figure 16. Test Minutes Required for Components to Fail (Test Vehicle 74 Data)

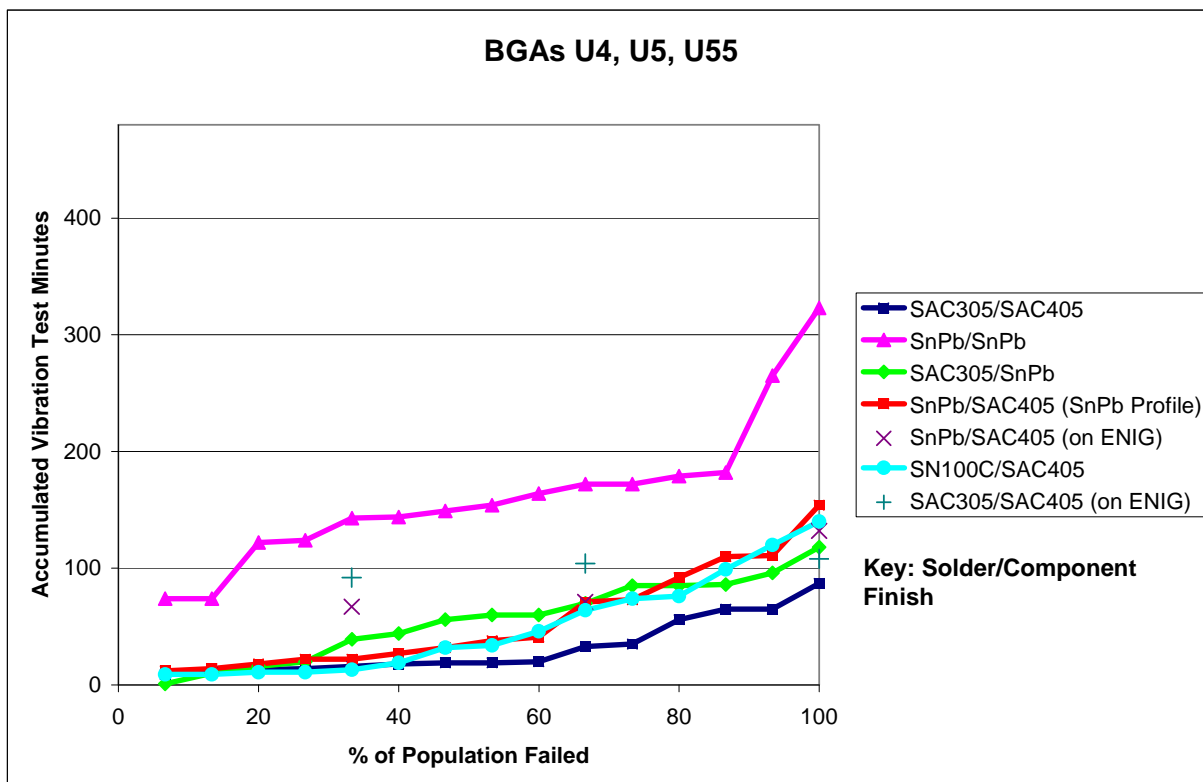


Figure 17. Combined Data from BGA's U4, U5, and U55

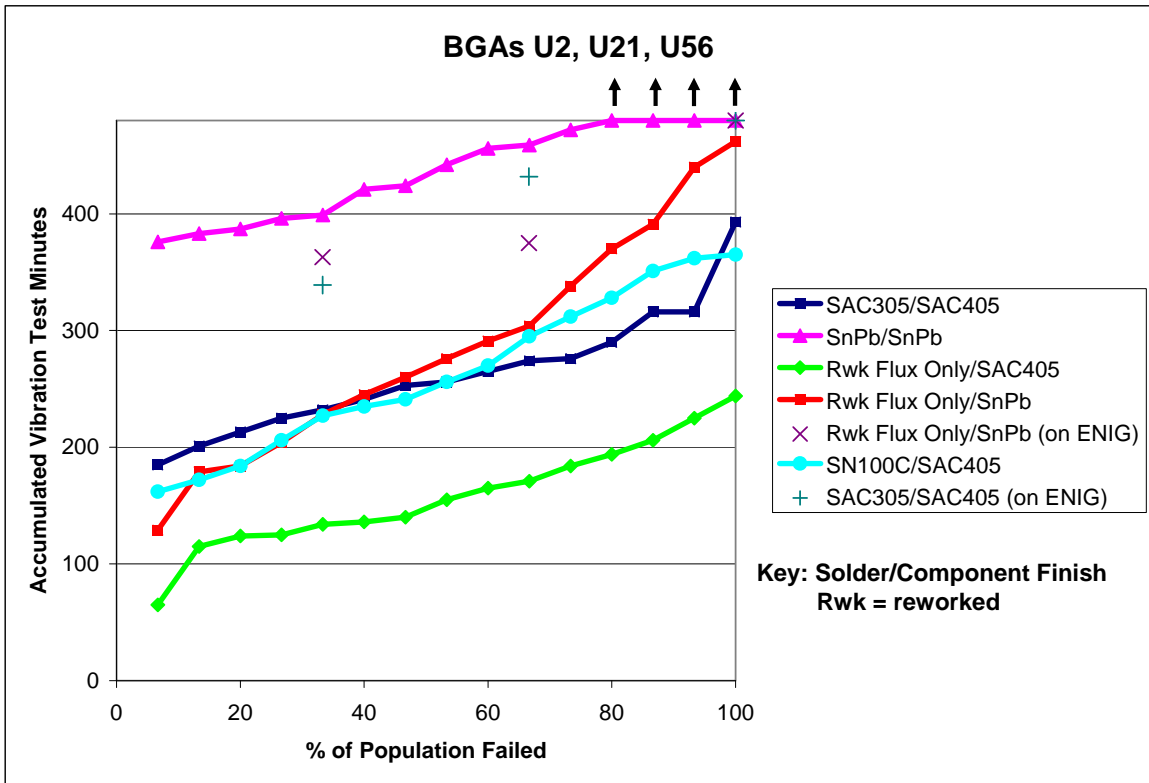


Figure 18. Combined Data from BGA's U2, U21, and U56

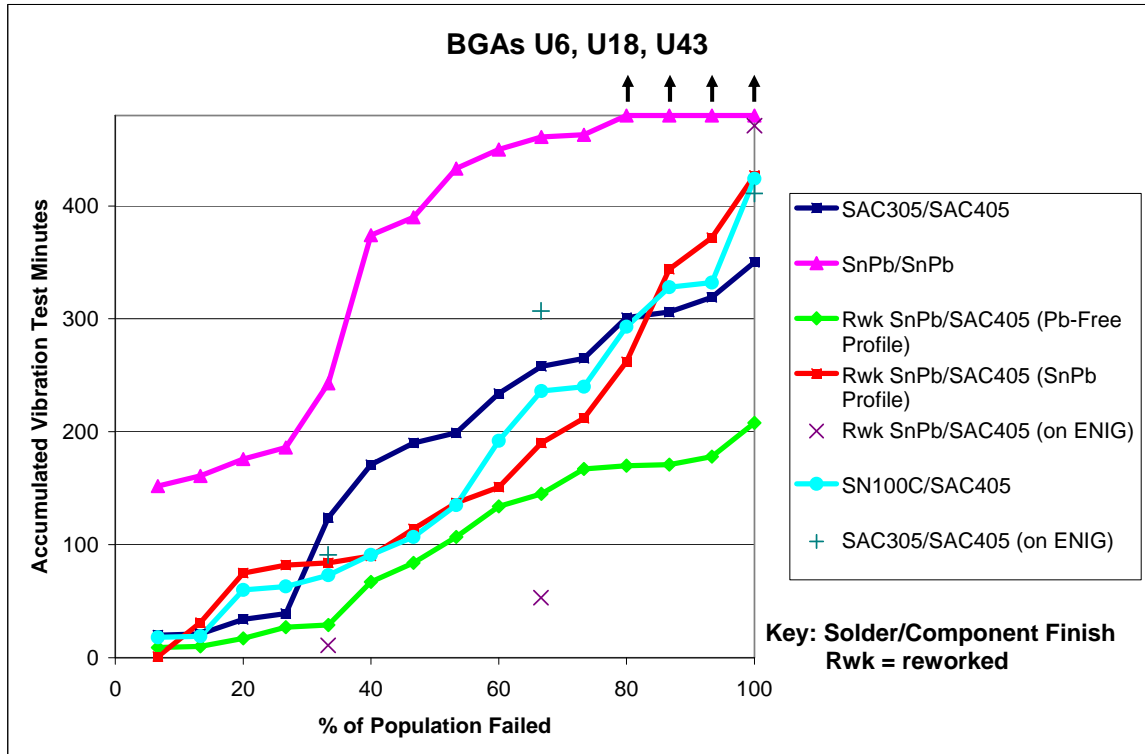
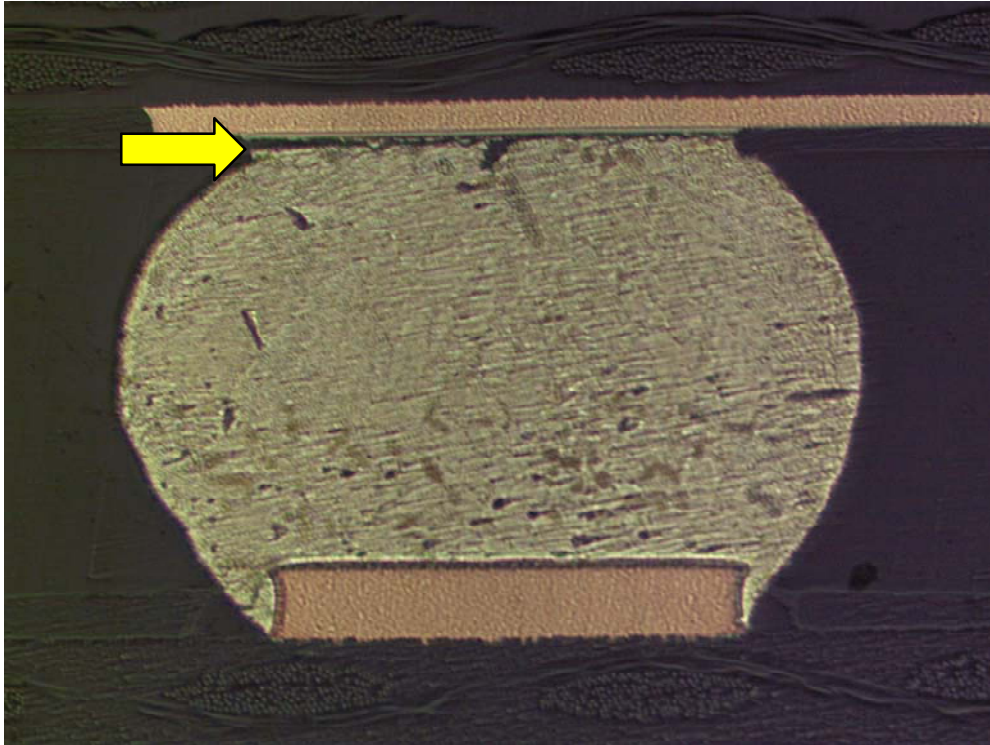
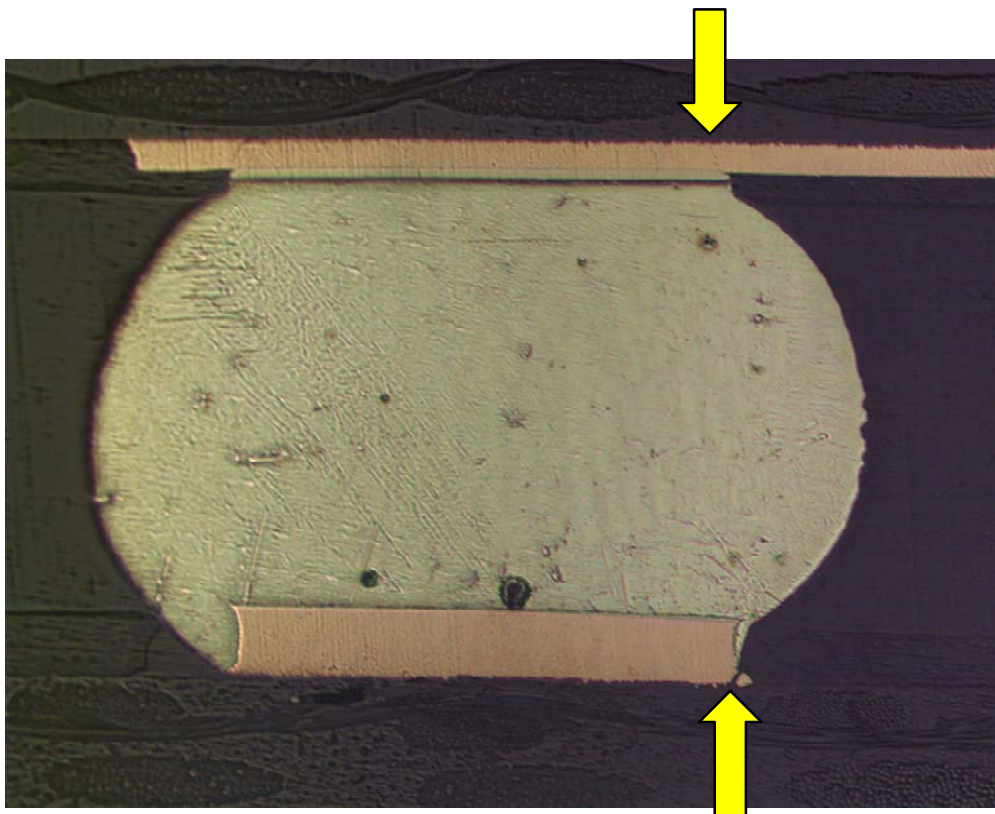


Figure 19. Combined Data from BGA's U6, U18, and U43



**Figure 20.** Test Vehicle 15 - Corner Ball of BGA U21 (SnPb Solder/SnPb Balls)



**Figure 21.** Test Vehicle 36 - Corner Ball of BGA U21 (SAC305 Solder/SAC405 Balls)

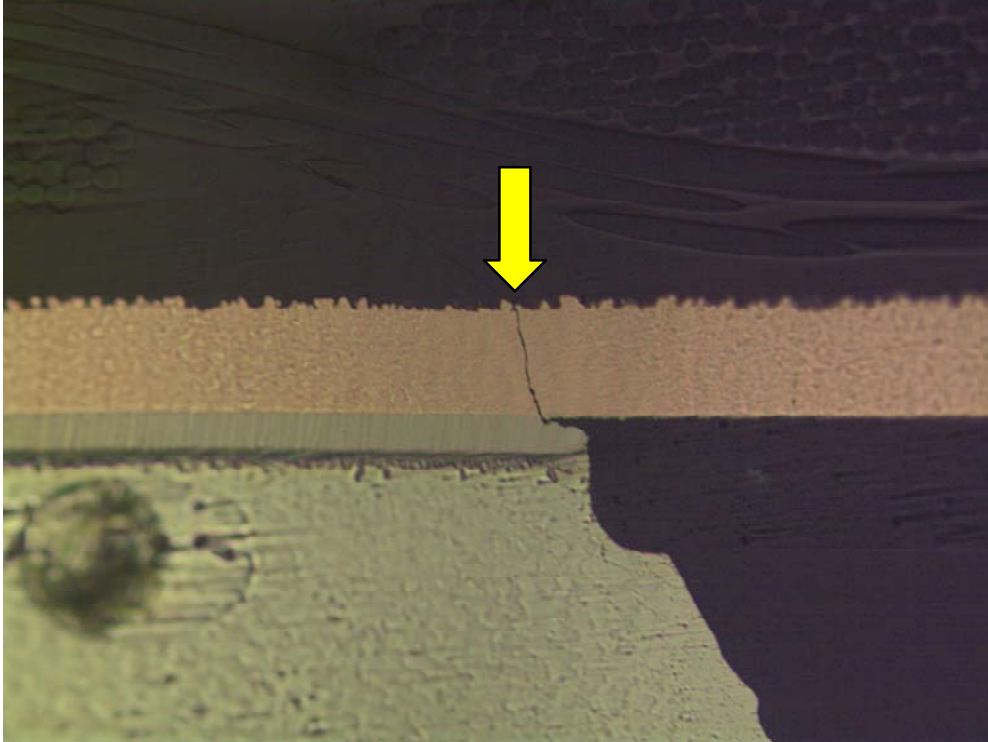


**Figure 22.** Test Vehicle 36 – Trace Crack on Component Side of BGA U21 (SAC305 Solder/SAC405 Balls)

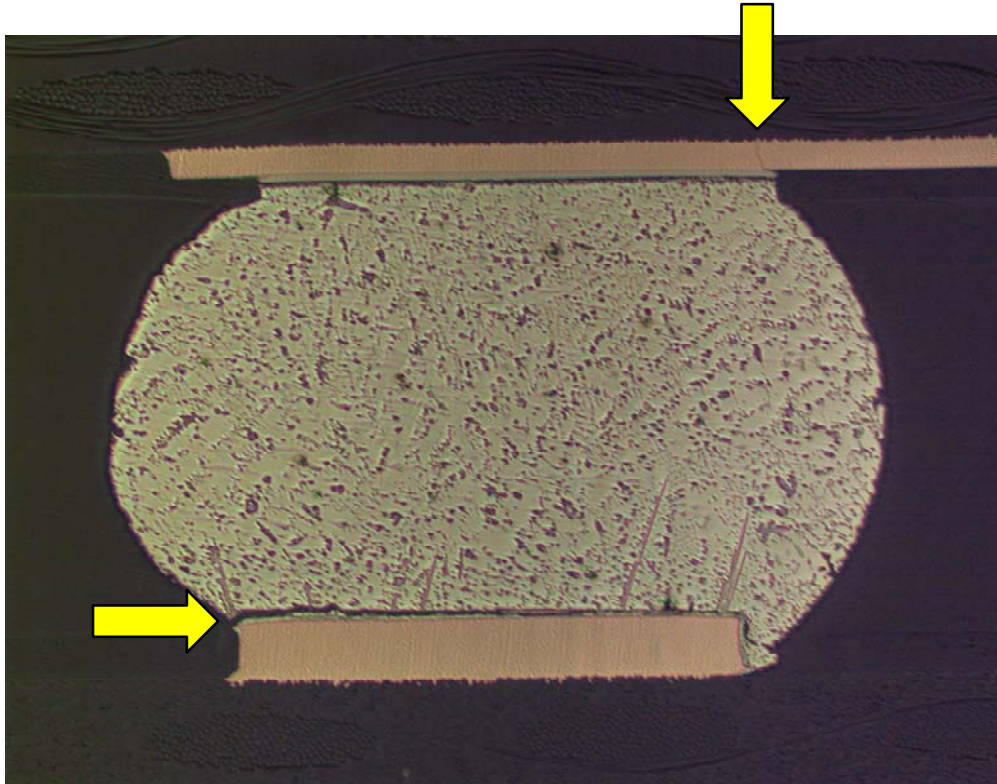


**Figure 23.** Test Vehicle 134 - Corner Ball of BGA U44 (SnPb Solder/SAC405 Balls)

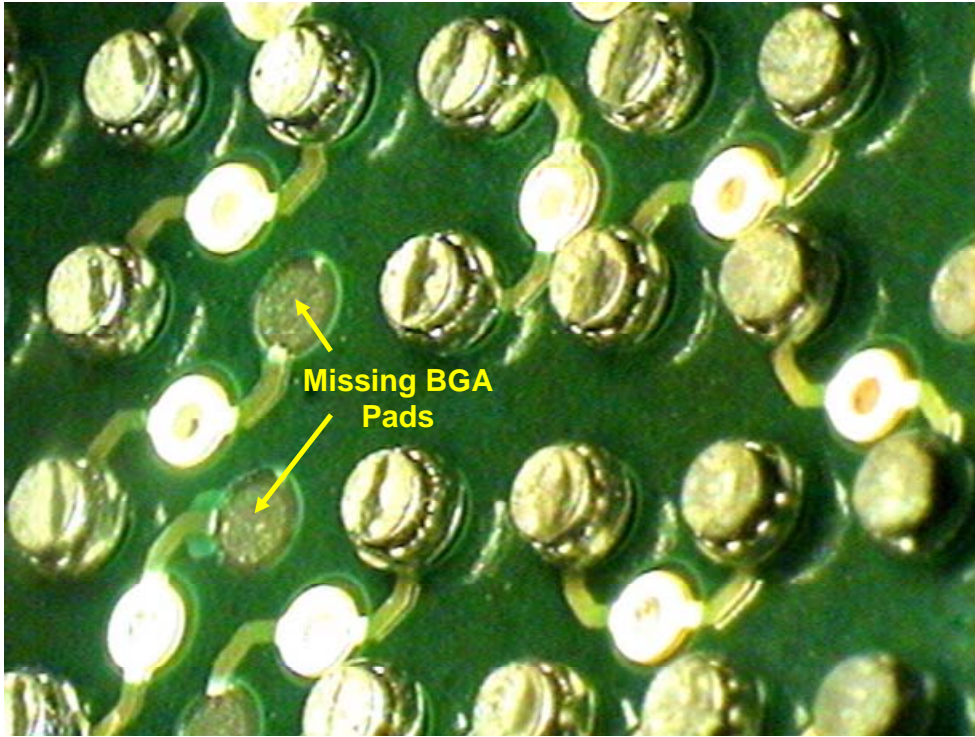


Figure 24. Test Vehicle 16 BGA U5 (SnPb Solder/SnPb Balls)

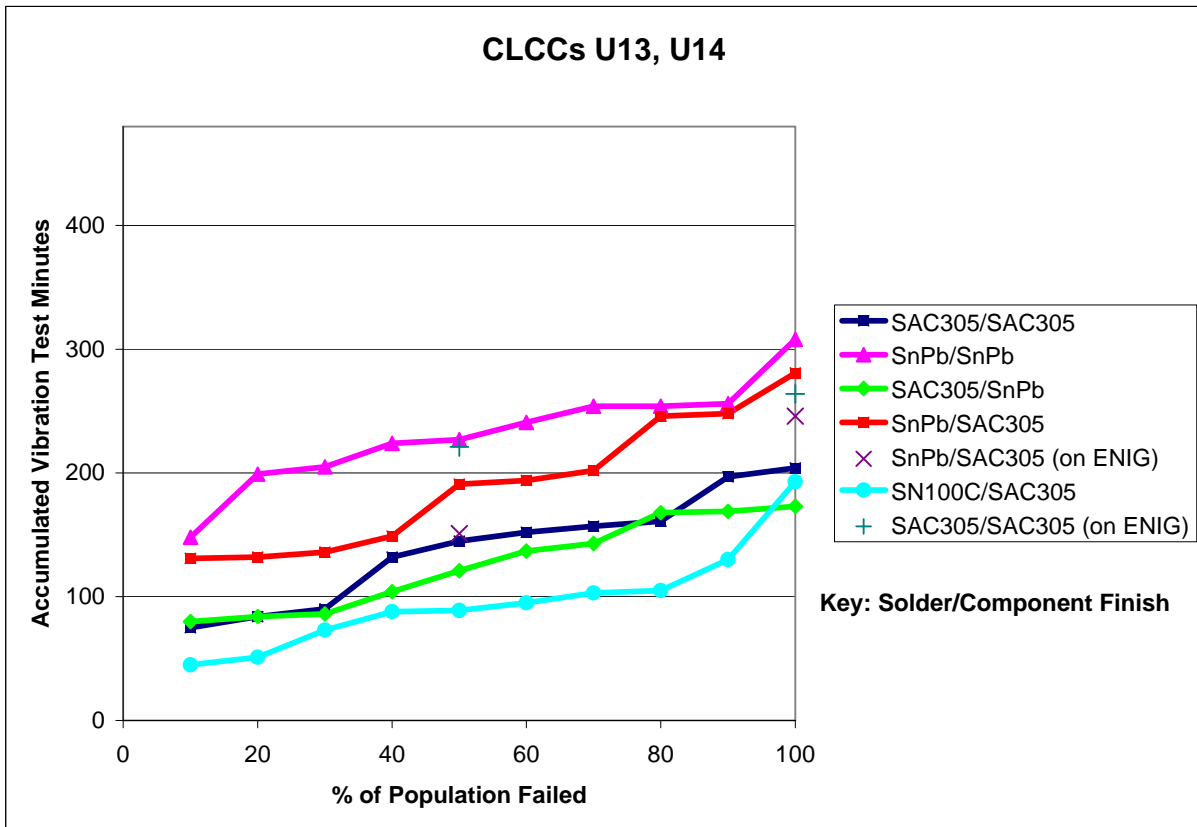


Figure 25. Combined Data from CLCC's U13 and U14

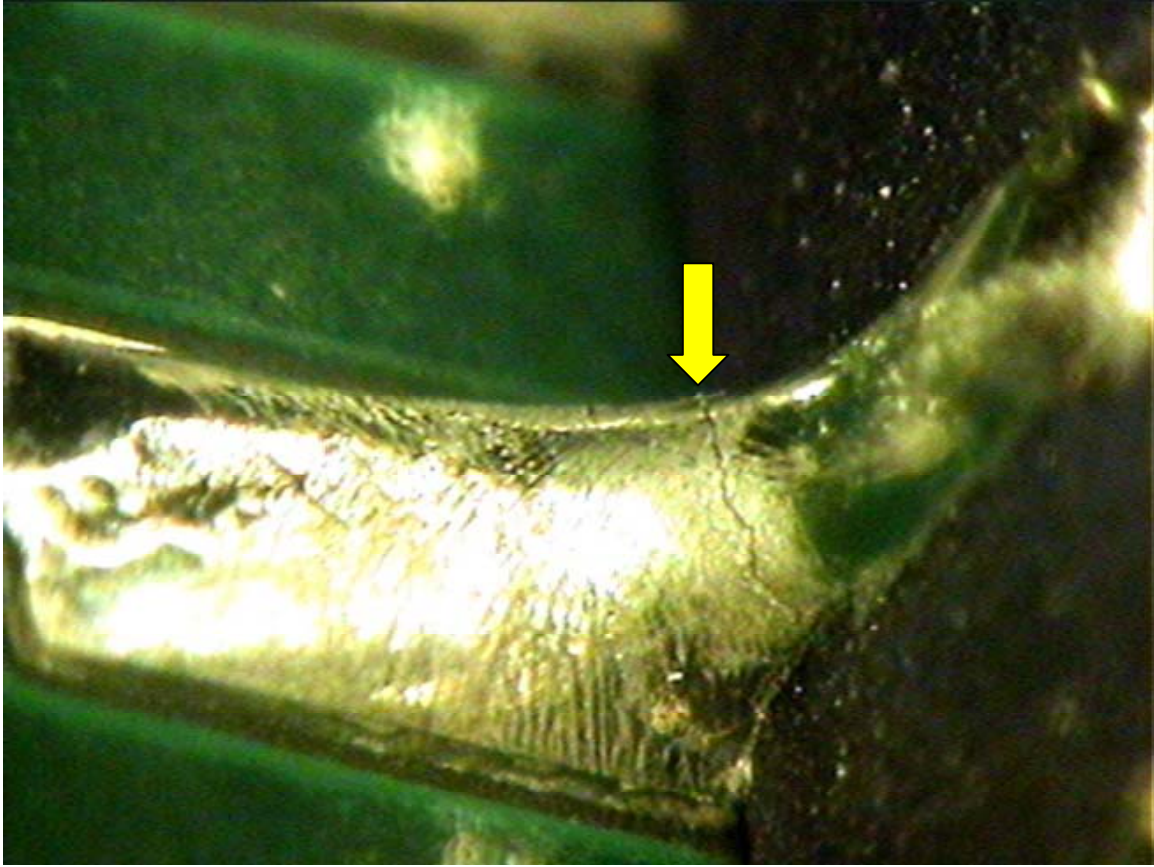


Figure 26. Test Vehicle 78 CLCC U14 (Cracked SAC305/SAC305 Solder Joint)

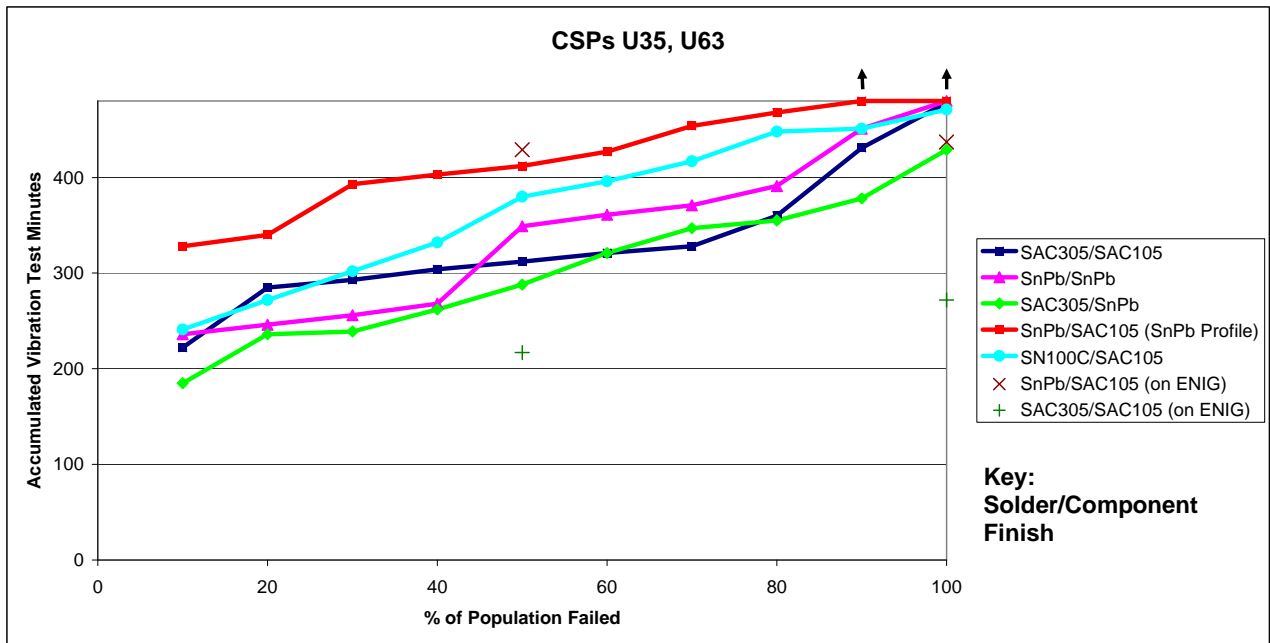


Figure 27. Combined Data from CSP U35, U63 Data

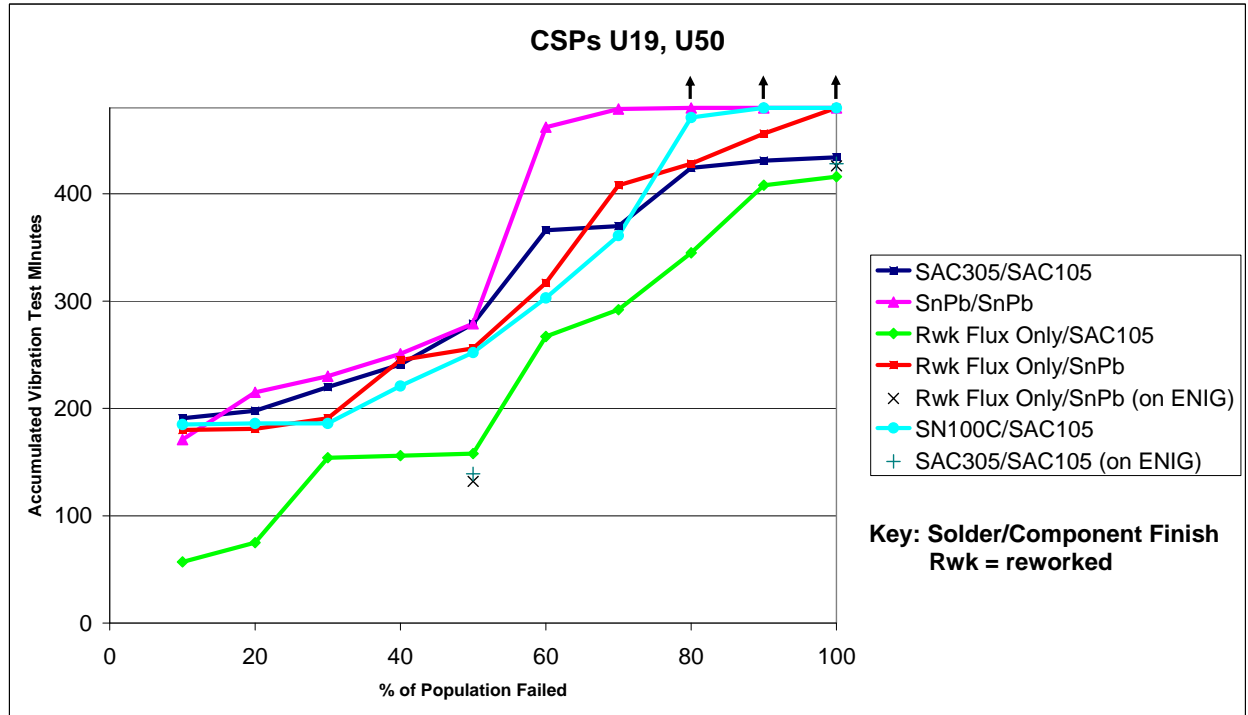


Figure 28. Combined Data from CSP's U19 and U50

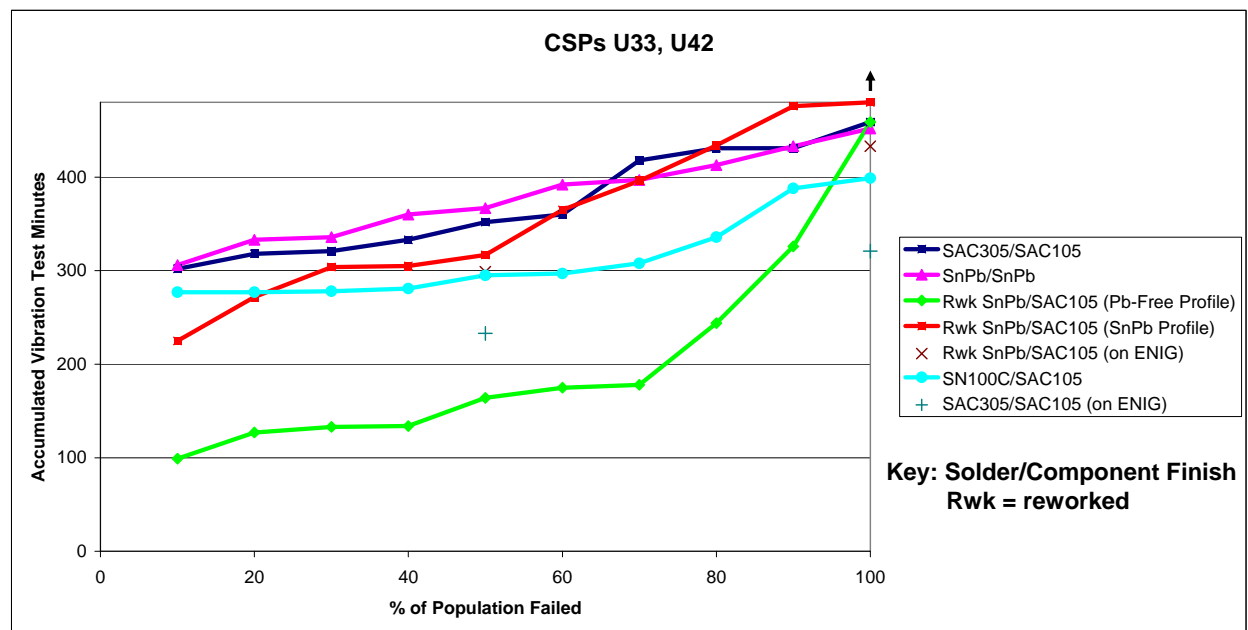
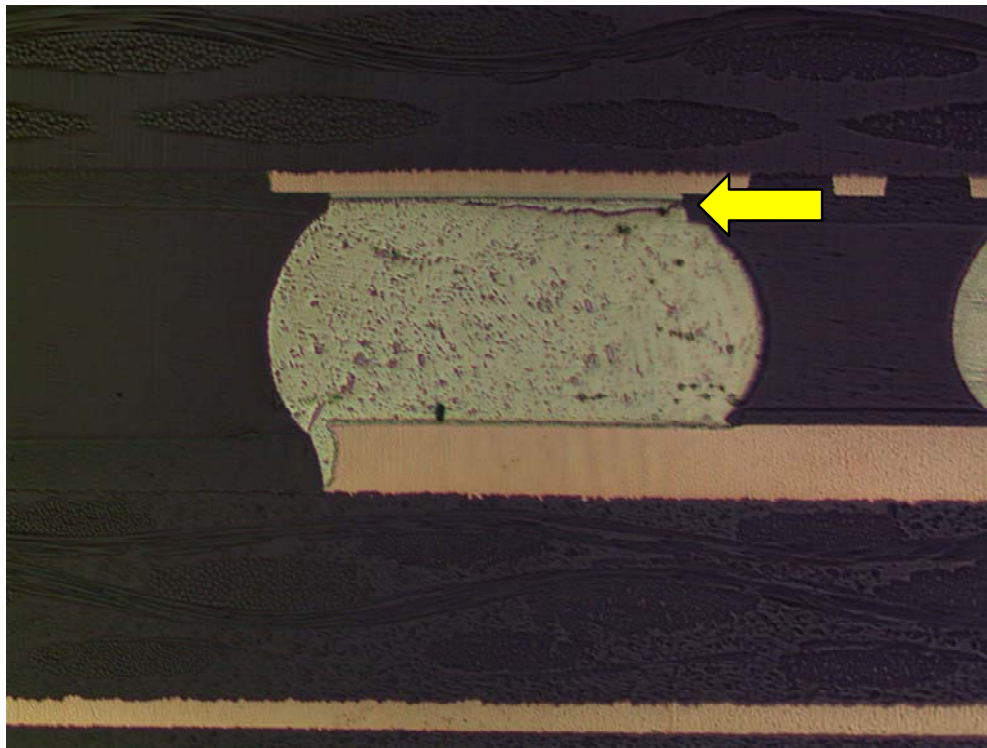
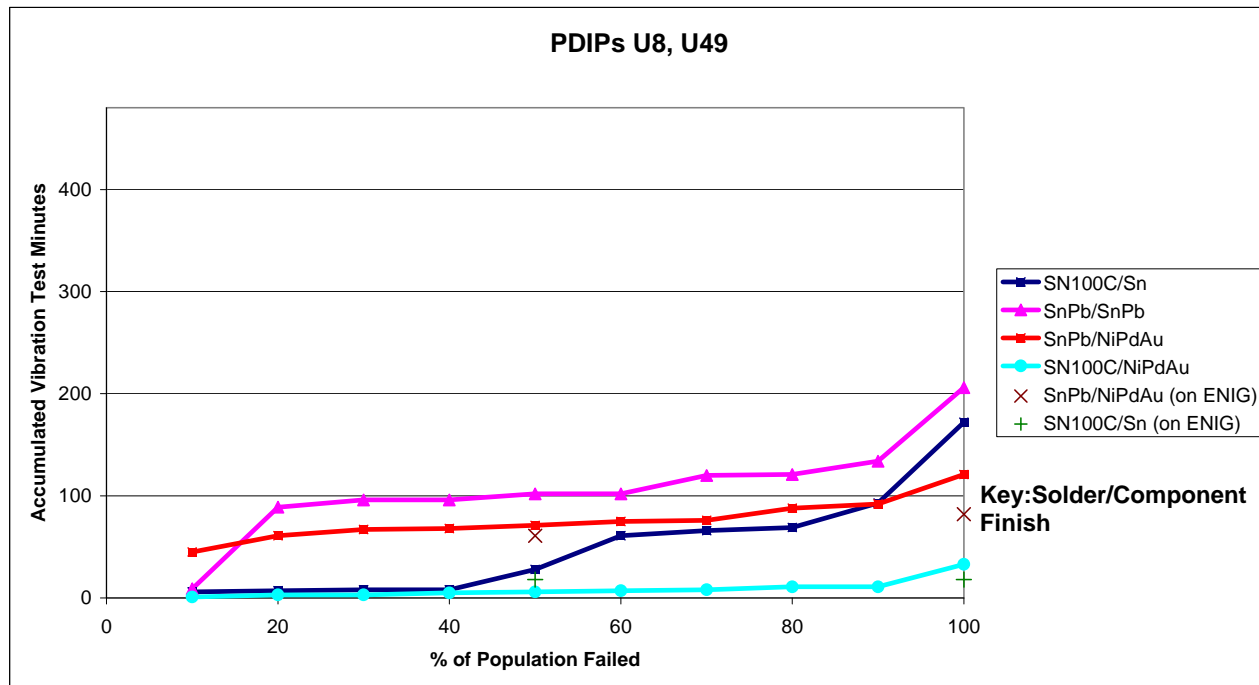


Figure 29. Combined Data from CSP's U33 and U42



**Figure 30.** Test Vehicle 36 – Corner Ball of CSP U35 (SAC305 Solder/SAC105 Balls)



**Figure 31.** Combined Data from PDIP's U8 and U49

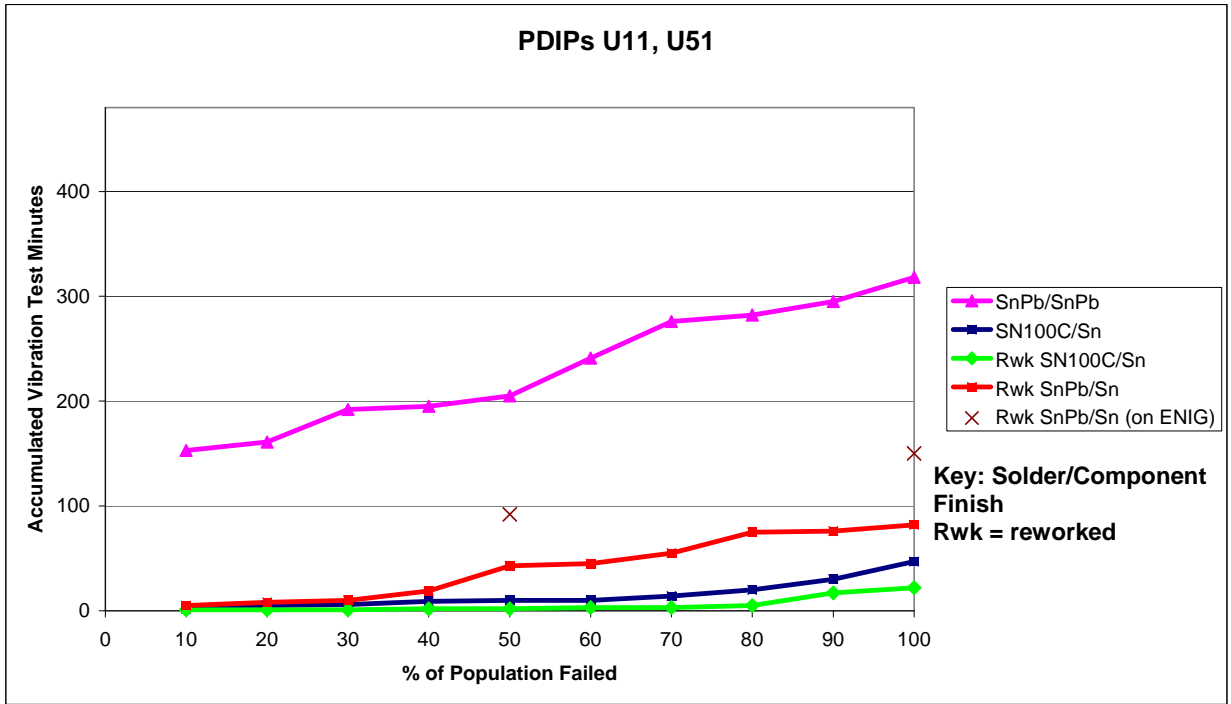


**Figure 32.** Combined Data from PDIP's U11 and U51

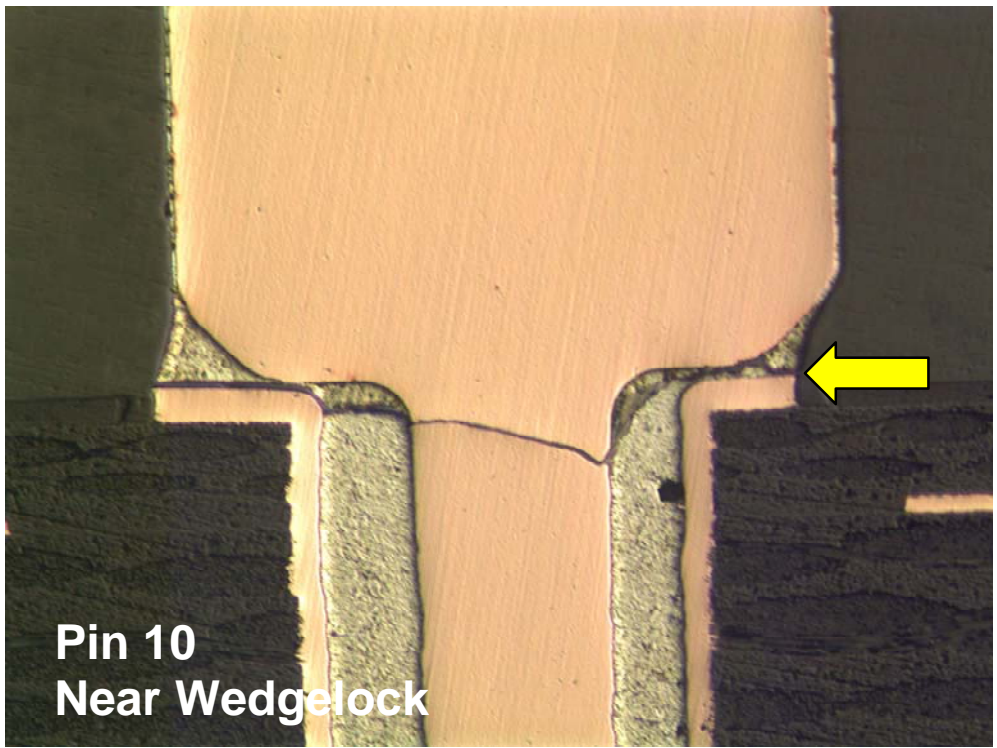


**Figure 33.** Test Vehicle 175 – Corner Lead of PDIP U51 (Reworked SN100C Solder/Sn Finish)

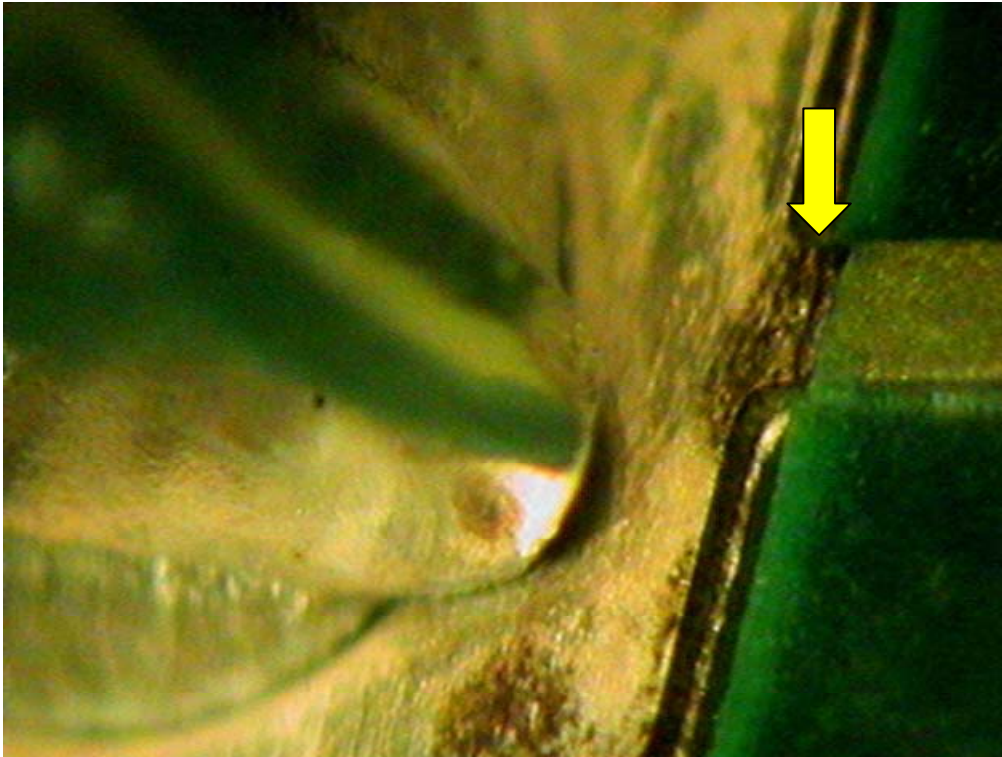


**Figure 34.** Test Vehicle 112 – Cracked Trace at Corner of PDIP U38 (SN100C/Sn)

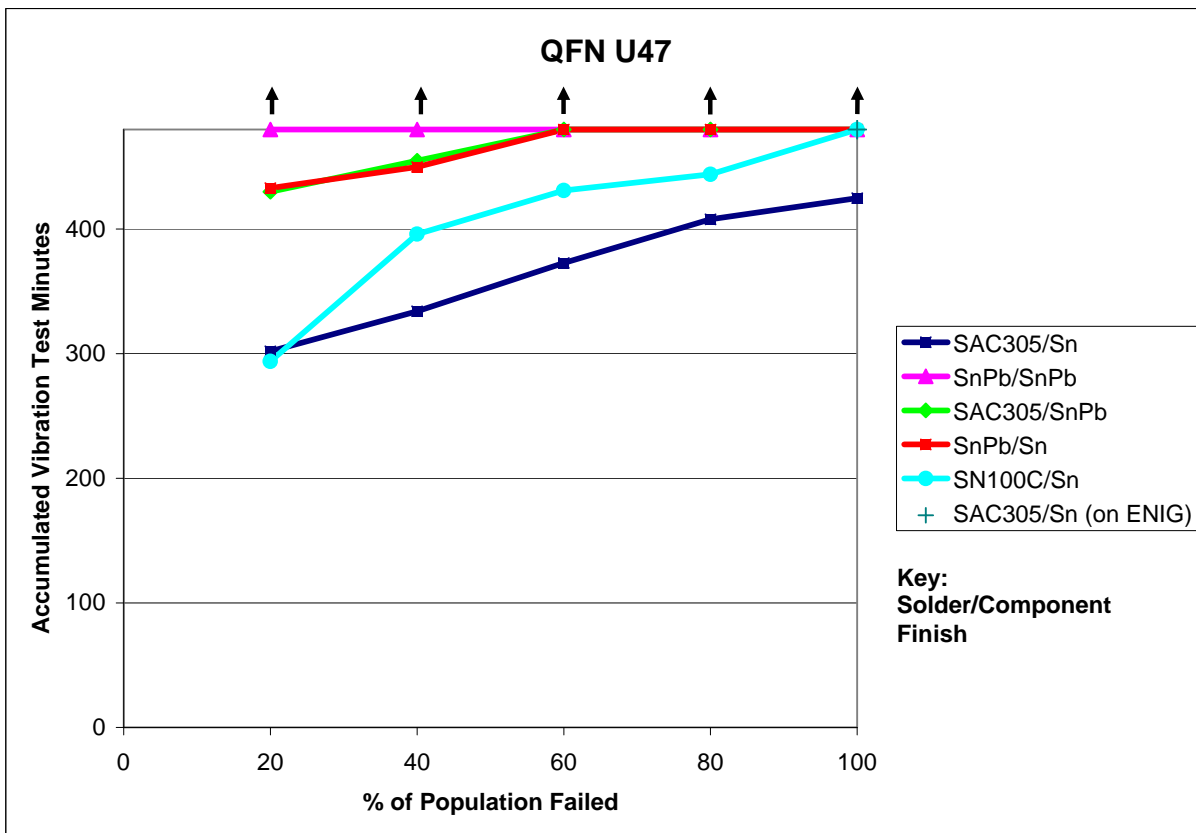


**Figure 35.** Data from QFN U47

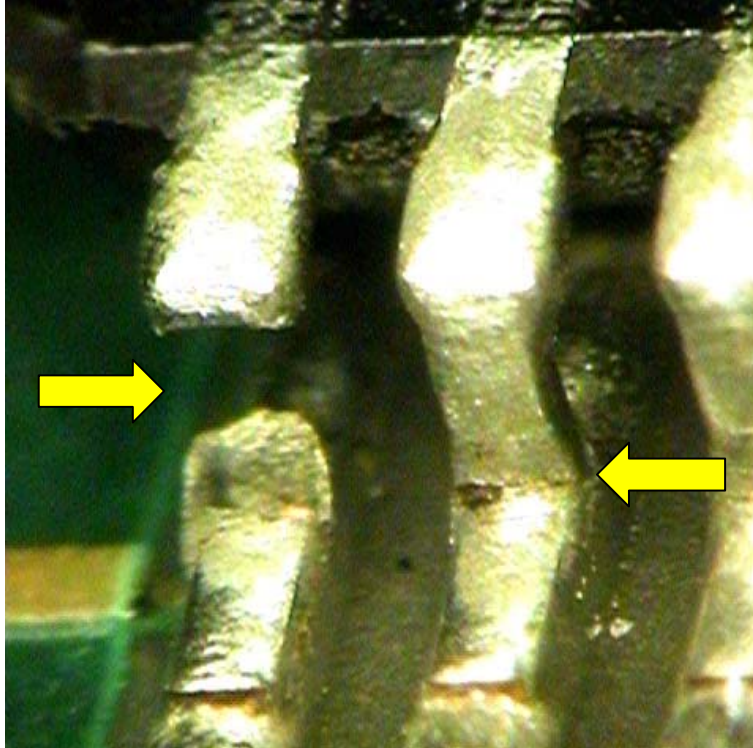


**Figure 36.** Test Vehicle 16 – Cracked Leads and Missing Lead on TQFP U58 (SnPb/Sn)

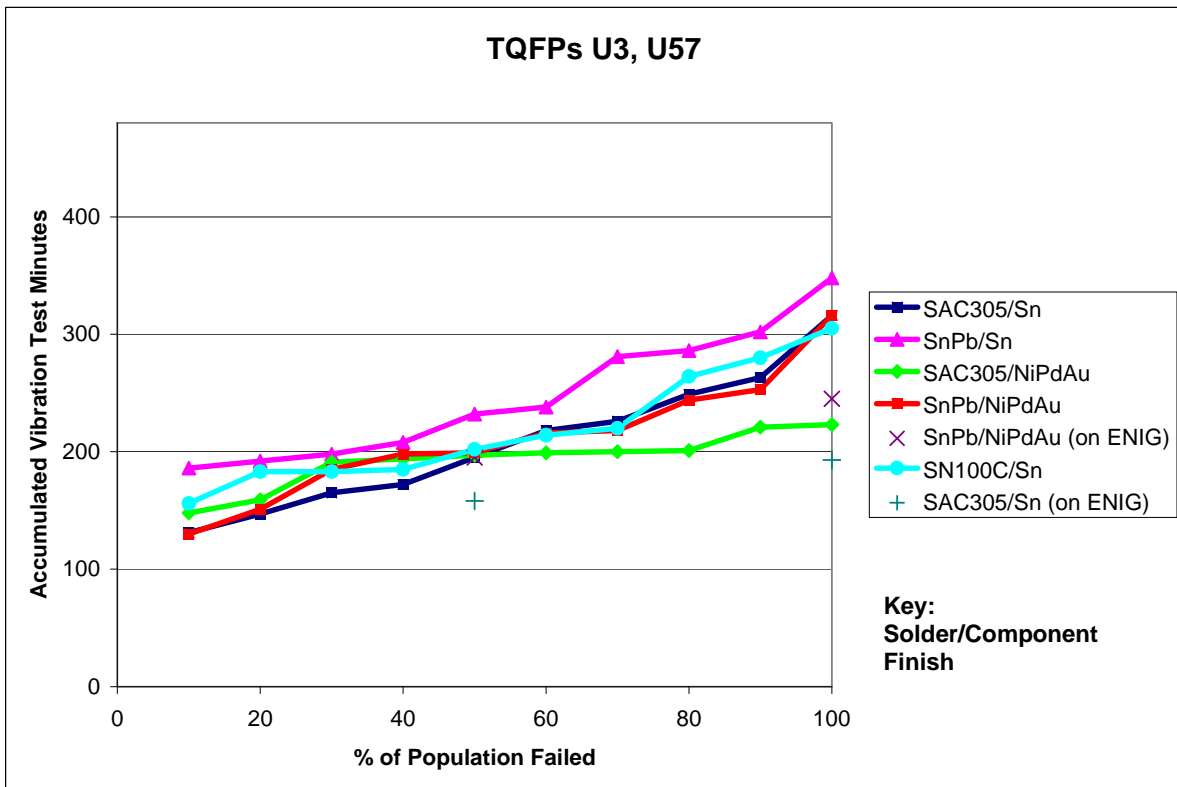


**Figure 37.** Combined Data from TQFP's U3 and U57

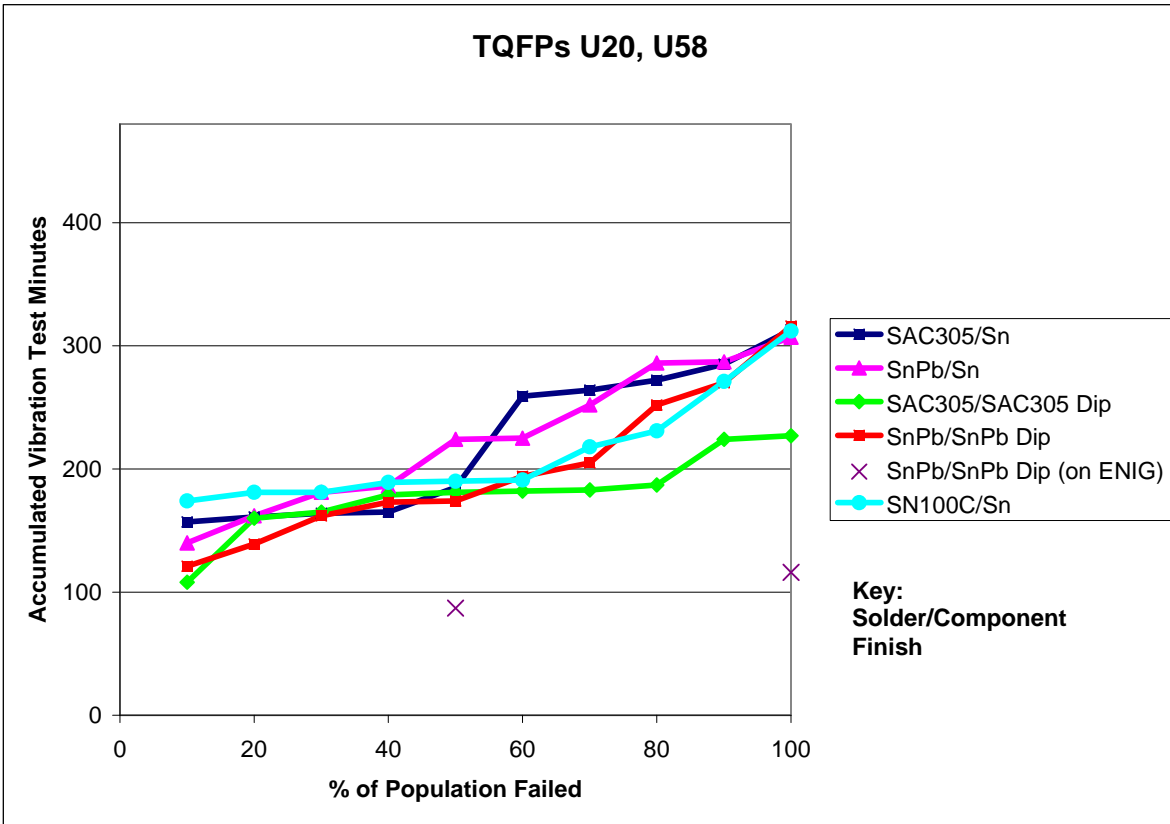


Figure 38. Combined Data from TQFP's U20 and U58

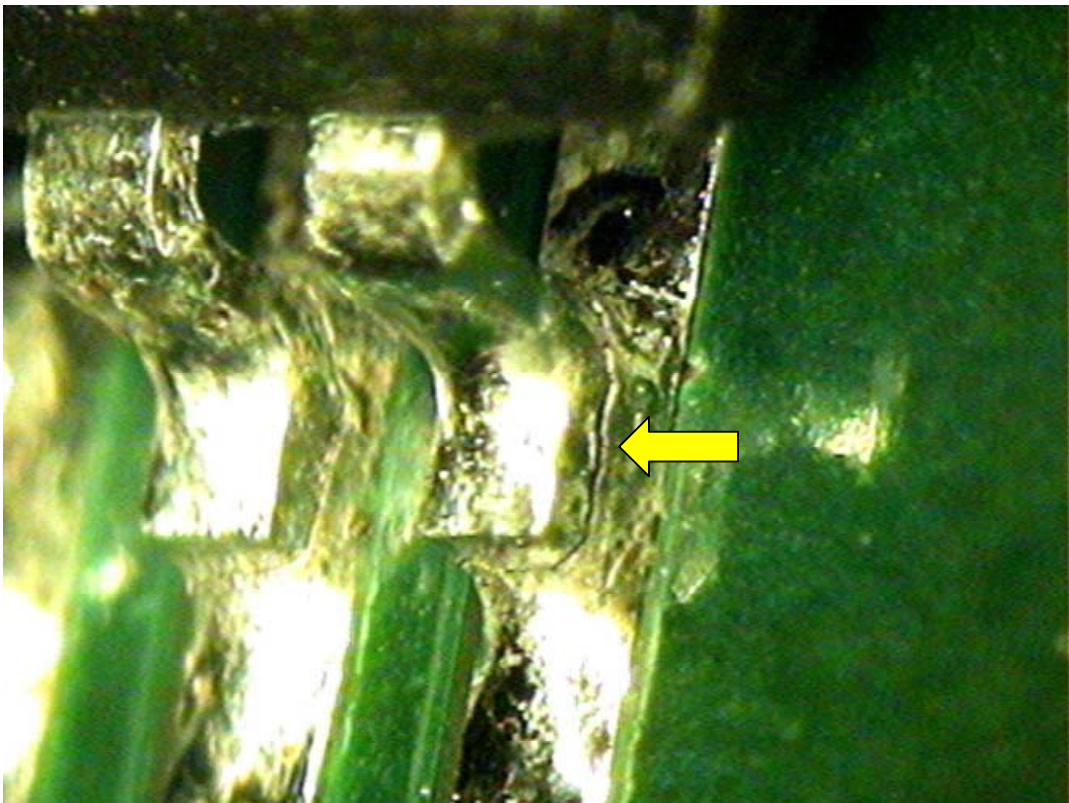


Figure 39. Test Vehicle 36 – Cracked Solder Joint on TSOP U25 (SAC305/Sn)

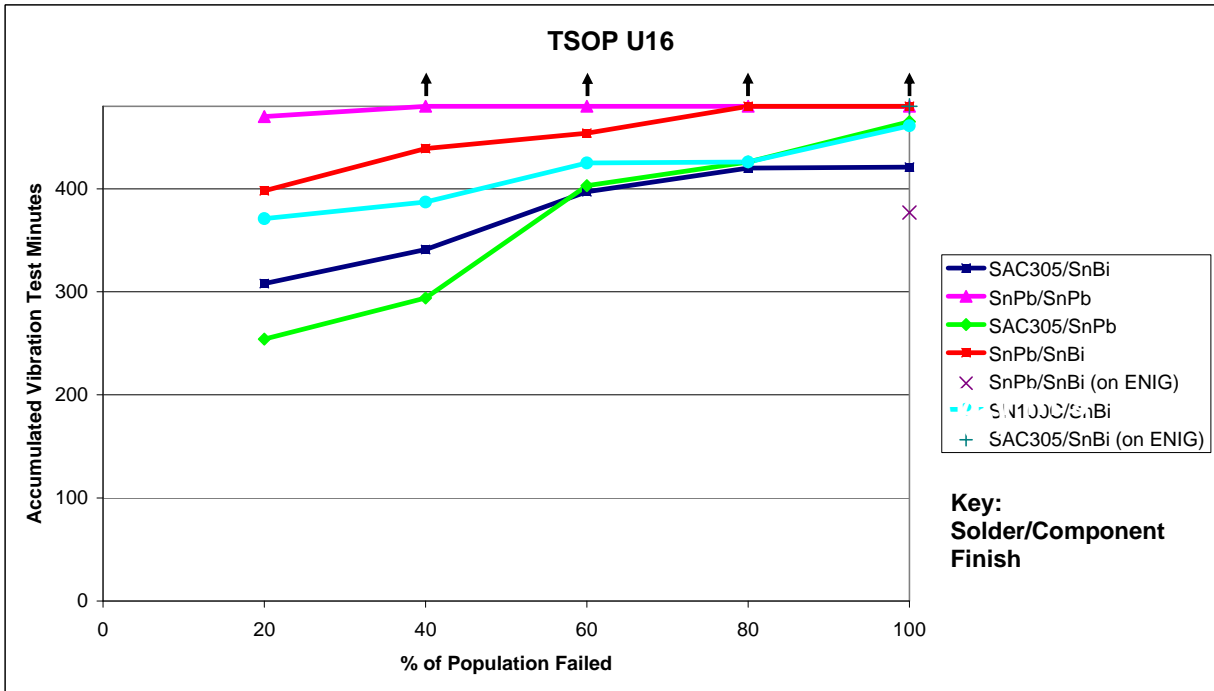


Figure 40. TSOP U16 Data

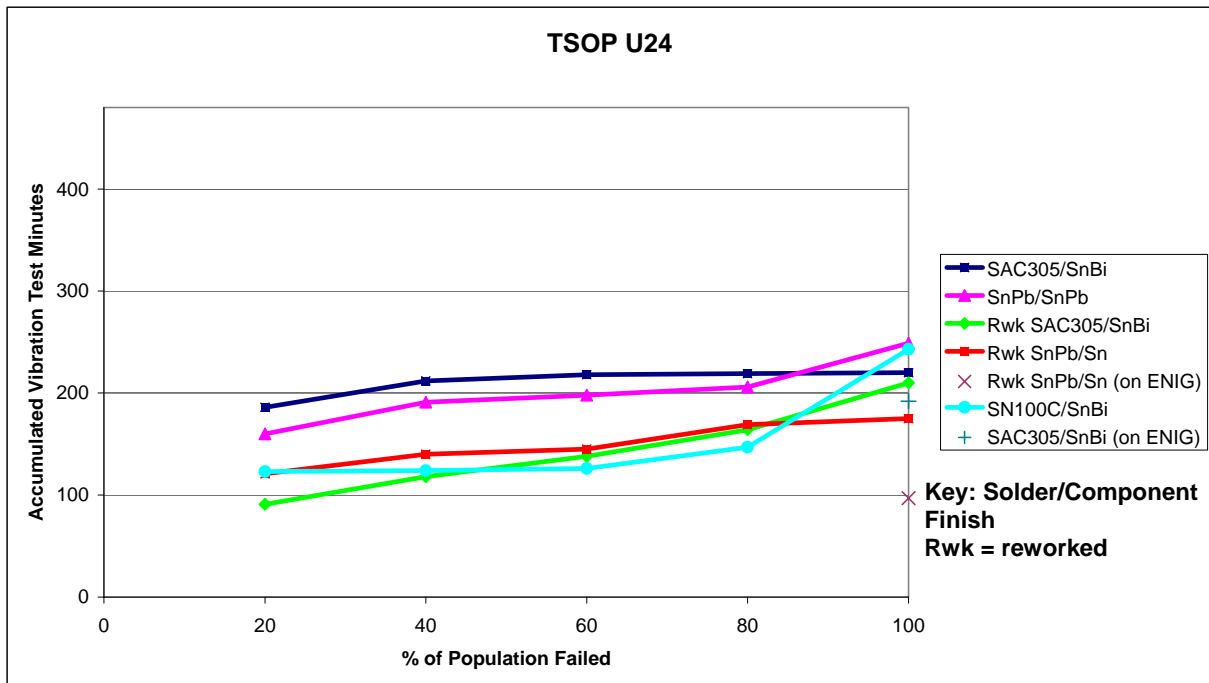


Figure 41. TSOP U24 Data

**Table 6.** Ranking of Solder Alloy/Component Finish Combinations

Relative Ranking (Solder/Finish)												
Component	Sn37Pb/Sn37Pb	SAC305/SAC405	Sn37Pb/SAC405	SAC305/Sn37Pb	Rwk Flux Only/Sn37Pb	Rwk Flux Only/SAC405	Rwk Sn37Pb/SAC405 (SnPb Profile)	Rwk Sn37Pb/SAC405 (Pb-Free Profile)	SN100C/SAC405			
BGA-225	1	3	3	3	3	3	3	3	3			
Component	Sn37Pb/Sn37Pb	SAC305/SAC305	Sn37Pb/SAC305	SAC305/Sn37Pb	SN100C/SAC305							
CLCC-20	1	3	2	3	3							
Component	Sn37Pb/Sn37Pb	SAC305/SAC105	Sn37Pb/SAC105	SAC305/Sn37Pb	Rwk Flux Only/Sn37Pb	Rwk Flux Only/SAC105	Rwk Sn37Pb/SAC105 (SnPb Profile)	Rwk Sn37Pb/SAC105 (Pb-Free Profile)	SN100C/SAC105			
CSP-100	1	1	1	2	1	2	1	3	1			
Component	Sn37Pb/SnPb	SN100C/Sn	Sn37Pb/NiPdAu	Rwk Sn37Pb/Sn	Rwk SN100C/Sn	SN100C/NiPdAu						
PDIP-20	1	3	2	3	3	3						
Component	Sn37Pb/Sn37Pb	SAC305/Sn	Sn37Pb/Sn	SAC305/Sn37Pb	SN100C/Sn							
QFN-20	1	2	1	1	2							
Component	Sn37Pb/Sn	SAC305/Sn	Sn37Pb/NiPdAu	SAC305/NiPdAu	Sn37Pb/Sn37Pb Dip	SAC305/SAC305 Dip	SN100C/Sn					
TQFP-144	1	1	1	2	1	2	1					
Component	Sn37Pb/SnPb	Sn37Pb/Sn	Sn37Pb/SnBi	SAC305/Sn	SAC305/SnBi	SAC305/SnPb	Rwk Sn37Pb/SnPb	Rwk Sn37Pb/Sn (SnPb Profile)	Rwk Sn37Pb/Sn (Pb-Free Profile)	Rwk SAC305/SnBi	SN100C/Sn	SN100C/SnBi
TSOP-50	1	2*	2*	2*	2*	2	2	2*	2	2	2	2

Key: Solder/Component Finish  
 Rwk = reworked  
 1 = as good as or better than Sn37Pb control  
 2 = worse than Sn37Pb control  
 3 = much worse than Sn37Pb control

\*Performance relative to Sn37Pb control may depend on orientation of the TSOP